



저작자표시-비영리-변경금지 2.0 대한민국

이용자는 아래의 조건을 따르는 경우에 한하여 자유롭게

- 이 저작물을 복제, 배포, 전송, 전시, 공연 및 방송할 수 있습니다.

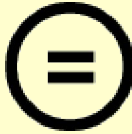
다음과 같은 조건을 따라야 합니다:



저작자표시. 귀하는 원저작자를 표시하여야 합니다.



비영리. 귀하는 이 저작물을 영리 목적으로 이용할 수 없습니다.



변경금지. 귀하는 이 저작물을 개작, 변형 또는 가공할 수 없습니다.

- 귀하는, 이 저작물의 재이용이나 배포의 경우, 이 저작물에 적용된 이용허락조건을 명확하게 나타내어야 합니다.
- 저작권자로부터 별도의 허가를 받으면 이러한 조건들은 적용되지 않습니다.

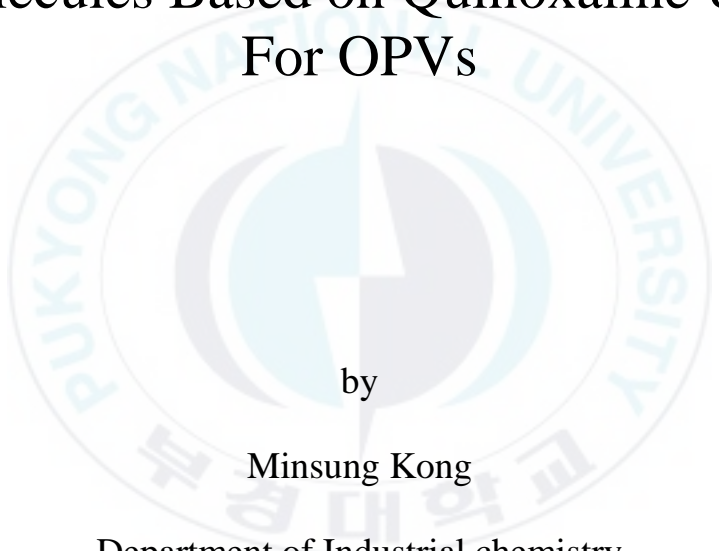
저작권법에 따른 이용자의 권리는 위의 내용에 의하여 영향을 받지 않습니다.

이것은 [이용허락규약\(Legal Code\)](#)을 이해하기 쉽게 요약한 것입니다.

[Disclaimer](#)

Thesis for the Degree of Master of Engineering

Synthesis and Characterization of New Type  
A-A Conjugated Copolymers and Small  
Molecules Based on Quinoxaline Unit  
For OPVs

The logo of Pukyong National University is a circular emblem. It features a central stylized design with a blue and grey color scheme, possibly representing a sun or a compass. The words "PUKYONG NATIONAL UNIVERSITY" are written in a circular path around the center. Below the English text, there is Korean text: "부경대학교".

by

Minsung Kong

Department of Industrial chemistry

The Graduate School

Pukyong National University

February 2017

# Synthesis and Characterization of New Type A-A Conjugated Copolymers and Small Molecules Based on Quinoxaline Unit For OPVs

(OPV 를 위한 Quinoxaline 을 기반으로 한 새로운 타입의 A-A 교대구조를 가지는 공액중합체와 단분자들의 합성과 특성)

Advisor: Prof. Youngeup Jin

by  
Minsung Kong

A thesis submitted in partial fulfillment of the requirements  
for the degree of

Master of Engineering

in Department of Industrial Chemistry, The Graduate School,  
Pukyong National University

February 2017

Synthesis and Characterization of New Type A-A Conjugated  
Copolymers and Small Molecules Based on  
Quinoxaline Unit  
For OPVs

A dissertation

by

Minsung Kong

Approved by:

---

(Seong Soo Park)

---

(Dong Wook Jang )

---

(Youngeup Jin)

February 2017

## Contents

Contents .....	i
List of Figures .....	viii
List of Tables .....	xi
List of Schemes .....	xii
Abstract .....	xiv
Chapter I. Introduction .....	1
I-1. The Background of Polymer Solar Cells (PSCs) and Small Molecule Solar Cells (SMSCs).....	1
I-2. Operating Mechanism of Device .....	3
I-3. Bulk Heterojunction Structure .....	4

I-4. Parameters of PSCs .....	6
I-4-1. Open-Circuit Voltage ( $V_{oc}$ ) .....	6
I-4-2. Short-Circuit Current Density ( $J_{sc}$ ) .....	7
I-4-3. Fill Factor ( $FF$ ) .....	8
I-5. Tactics to Synthesize Conjugated Polymers for High Performance .....	9
I-5-1. Acceptor-Acceptor (A-A) Type Polymer.....	9
I-5-2. Small Molecule.....	10
I-5-3. Influence of Functionalities Substitution in Conjugated Backbone.....	11
I-5-4. Selection of Donor and Acceptor Unit in Conjugated Materials.....	12
Chapter II. Experimental .....	14
II-1. Materials and Instruments .....	14
II-2. Synthesis of monomers .....	16
II-2-1. Synthesis of donor monomers .....	16
II-2-1-1. Synthesis of thiophene-3-carbonyl chloride .....	16
II-2-1-2. Synthesis of <i>N,N</i> -diethylthiophene-3-carboxamide .....	16

II-2-1-3. Synthesis of benzo[1,2- <i>b</i> :4,5- <i>b'</i> ]dithiophene-4,8-dione .....	17
II-2-1-4. Synthesis of 4,8-bis(2-ethylhexyloxy)benzo[1,2- <i>b</i> :4,5- <i>b'</i> ]dithiophene .....	18
II-2-1-5. Synthesis of 2,6-bis(trimethyltin)-4,8-bis(2-ethylhexyloxy)benzo[1,2- <i>b</i> :3,4 <i>b'</i> ]dithiophene.....	18
II-2-1-6. Synthesis of 4,8-bis(octyloxy)benzo[1,2- <i>b</i> :4,5- <i>b'</i> ]dithiophene .....	19
II-2-1-7. Synthesis of 2,6-bis(trimethyltin)-4,8-bis(octyloxy)benzo[1,2- <i>b</i> :3,4- <i>b'</i> ]dithiophene.....	20
II-2-1-8. Synthesis of 2,5-bis(trimethylstannyl)thiophene.....	22
II-2-1-9. Synthesis of 5,5'-bis(trimethylstannyl)-2,2'-bithiophene.....	22
II-2-1-10. Synthesis of 2,5-bis-trimethylstannyl-thieno[3,2- <i>b</i> ]thiophene.....	23
II-2-1-11. Synthesis of 2,5-dibromothiophene.....	24
II-2-1-12. Synthesis of tributyl(thiophen-2-yl)stannane.....	24
II-2-1-13. Synthesis of 2,2':5',2''-terthiophene.....	25
II -2-1-14. Synthesis of 2,5''-bis(trimethylsilyl)-5,2',5',2''- terthiophene.....	25
II-2-1-15. Synthesis of tributyl(3-hexylthiophen-2-yl)stannane.....	28
II-2-2-16. Synthesis of tributyl(4-hexylthiophen-2-yl)stannane.....	28

II-2-1-17. Synthesis of tributyl(thieno[3,2- <i>b</i> ]thiophen-2-yl)stanne.....	29
II-2-2. Synthesis of acceptor monomers .....	31
II-2-2-1. Synthesis of 2,3-difluoro-1,4-bis-(trimethylsilyl)benzene .....	31
II-2-2-2. Synthesis of 1,4-dibromo-2,3-difluoro-benzene.....	31
II-2-2-3. Synthesis of 1,4-dibromo-2,3-difluoro-5,6-dinitro-benzene.....	32
II-2-2-4. Synthesis of 3,6-dibromo-4,5-difluorobenzene-1,2-diamine.....	32
II-2-2-5. Synthesis of hexacosane-13,14-dione.....	33
II-2-2-6. Synthesis of 5,8-dibromo-6,7-difluoro-2,3-didodecylquinoxaline.....	34
II-2-2-7. Synthesis of tetradecane-7,8-dione.....	36
II-2-2-8. Synthesis of 5,8-dibromo-6,7-difluoro-2,3-dihexylquinoxaline.....	37
II-2-2-9. Synthesis of 2,3-didodecyl-6,7-difluoro-5,8-di(thiophen-2-yl)quinoxaline.....	38
II-2-2-10. Synthesis of 5,8-bis(5-bromothiophen-2-yl)-2,3-didodecyl-6,7-difluoroquinoxaline.....	38
II-2-2-11. Synthesis of 5-(5-bromothiophen-2-yl)-2,3-didodecyl-6,7-difluoro-8-(thiophen-2-yl)quinoxaline.....	39
II-2-2-12. Synthesis of 6,7-difluoro-2,3-dihexyl-5,8-di(thiophen-2-yl)quinoxaline.....	40

II-2-2-13. Synthesis of 5-(5-bromothiophen-2-yl)-2,3-dihexcyl-6,7-difluoro-8-(thiophen-2-yl)quinoxaline.....	40
II-3. Synthesis of polymers .....	42
II-3-1. Synthesis of poly[4,4'-dibutoxy-2-(2,3-didodecyl-6,7-difluoro-8-phenylquinoxaline-5-yl)-2'-phenyl-5,5'-bithiazole] (YJ-61).....	42
II-3-2. Synthesis of poly[4,4'-dibutoxy-2-(5-(2,3-didodecyl-6,7-difluoro-8-(5-phenylthiophen-2-yl)quinoxaline-5-yl)-2'-phenyl-5,5'-bithiazole] (YJ-62).....	44
II-4. Synthesis of small molecule.....	46
II-4-1. Synthesis of 5,8-di([2,2'-bithiophehene]-5-yl)-2,3-didodecyl-6,7-difluoroquinoxaline (YJ-63).....	46
II-4-2. Synthesis of 2,3-didodecyl-6,7-difluoro-5,8-bis(thieno[3,2-b]thiophen-2-yl)quinoxaline (YJ-64).....	48
II-4-3. Synthesis of 2,3-didodecyl-6,7-difluoro-5,8-bis(3''-hexyl-[2,2':5',2''-terthiophen]-5-yl)quinoxaline (YJ-65).....	50
II-4-4. Synthesis of 2,3-didodecyl-6,7-difluoro-5,8-bis(4''-hexyl-[2,2':5',2''-terthiophen]-5-yl)quinoxaline (YJ-66).....	52
II-4-5. Synthesis of 2,3-didodecyl-6,7-difluoro-5,8-bis(5-(3-hexylthiophen-2-	

	yl)thieno[3,2- <i>b</i> ]thiophen-2-yl)quinoxaline (YJ-67).....	54
II-4-6.	Synthesis of 2,3-didodecyl-6,7-difluoro-5,8-bis(5-(4-hexylthiophen-2-yl)thieno[3,2- <i>b</i> ]thiophen-2-yl)quinoxaline (YJ-68).....	56
II-4-7.	Synthesis of 5,5''-bis(2,3-didodecyl-6,7-difluoro-8-(thiophen-2-yl)quinoxalin-5-yl)-2,2':5',2'':5'',2'''-quaterthiophene (YJ-69).....	58
II-4-8.	Synthesis of 5-(4-(5-(5-(2,3-didodecyl-6,7-difluoro-8-(thiophen-2-yl)quinoxalin-5-yl)thiophen-2-yl)thieno[3,2- <i>b</i> ]thiophen-2-yl)thiophen-2-yl)2,3-didodecyl-6,7-difluoro-8-(thiophen-2-yl)quinoxaline (YJ-70)....	60
II-4-9.	Synthesis of 8,8'-(5,5'-(4,8-bis((2-ethylhexyl)oxy)benzo[1,2- <i>b</i> :4,5- <i>b</i> ']dithiophene-2,6-diyl)bis(thiophene-5,2-diyl))bis(2,3-didodecyl-6,7-difluoro-5-(thiophen-2-yl)quinoxaline (YJ-71).....	62
II-4-10.	Synthesis of 8,8'-(5,5'-(4,8-bis((2-ethylhexyl)oxy)benzo[1,2- <i>b</i> :4,5- <i>b</i> ']dithiophene-2,6-diyl)bis(thiophene-5,2-diyl))bis(2,3-dihexyl-6,7-difluoro-5-(thiophen-2-yl)quinoxaline (YJ-72).....	64
II-4-11.	Synthesis of 8,8'-(5,5'-(4,8-bis(octyloxy)benzo[1,2- <i>b</i> :4,5- <i>b</i> ']dithiophene-2,6-diyl)bis(thiophene-5,2-diyl))bis(2,3-didodecyl-6,7-difluoro-5-(thiophen-2-yl)quinoxaline (YJ-73).....	66
II-4-12.	Synthesis of 8,8'-(5,5'-(4,8-bis(octyloxy)benzo[1,2- <i>b</i> :4,5- <i>b</i> ']dithiophene-	

2,6-diyl)bis(thiophene-5,2-diyl))bis(2,3-dihexcyl-6,7-difluoro-5-(thiophen-2-yl)quinoxaline (YJ-74).....	68
Chapter III. Results and Discussion .....	70
III-1. Polymerization Results .....	70
III-2. Thermal Stability of Polymers and Small Molecules.....	71
III-3. Optical Properties of Polymers and Small Molecule.....	72
III-3-1. Optical Properties of Polymers.....	72
III-3-2. Optical Properties of Small Molecules.....	75
III-4. Electrochemical Properties of Materials .....	82
III-5. Photovoltaic Properties of Materials.....	88
Chapter IV. Conclusions .....	92
References .....	93

## List of Figures

Figure I -1. Detailed working mechanism of PSCs in heterojunction solar cells.

Figure I -2. Structures of bulk-heterojunction device.

Figure I -3. Acceptor-acceptor type polymer solar cells.

Figure I -4. Two types of organic solar materials.

Figure III-1. Thermo gravimetric analysis of materials.

Figure III-2. UV-visible absorption spectra of polymers in chloroform.

Figure III-3. UV-visible absorption spectra of polymers in a thin film formed via spin-cast from a solution in chloroform (1wt%).

Figure III-4. UV-visible absorption spectra of YJ-63, YJ-64 in chloroform.

Figure III-5. UV-visible absorption spectra of YJ-63, YJ-64 in a thin film formed via spin-cast from a solution in chloroform (1wt%).

Figure III-6. UV-visible absorption spectra of YJ-65, YJ-66 in chloroform.

Figure III-7. UV-visible absorption spectra of YJ-65, YJ-66 in a thin film formed via spin-cast from a solution in chloroform (1wt%).

Figure III-8. UV-visible absorption spectra of YJ-67, YJ-68 in chloroform.

Figure III-9. UV-visible absorption spectra of YJ-67, YJ-68 in a thin film formed via

spin-cast from a solution in chloroform (1wt%).

Figure III-10. UV-visible absorption spectra of YJ-69, YJ-70 in chloroform.

Figure III-11. UV-visible absorption spectra of YJ-69, YJ-70 in a thin film formed via spin-cast from a solution in chloroform (1wt%).

Figure III-12. UV-visible absorption spectra of YJ-71 ~ YJ-74 in chloroform.

Figure III-13. UV-visible absorption spectra of YJ-71 ~ YJ-74 in a thin film formed via spin-cast from a solution in chloroform (1wt%).

Figure III-14. Cyclic voltammetry curves of YJ-61, YJ-62 in 0.1 M  $\text{Bu}_4\text{NPF}_6$  acetonitrile solution at a scan rate of 100 mV/s at room temperature (vs an Ag quasi-reference electrode).

Figure III-15. Cyclic voltammetry curves of YJ-63, YJ-64 in 0.1 M  $\text{Bu}_4\text{NPF}_6$  acetonitrile solution at a scan rate of 100 mV/s at room temperature (vs an Ag quasi-reference electrode).

Figure III-16. Cyclic voltammetry curves of YJ-65, YJ-66 in 0.1 M  $\text{Bu}_4\text{NPF}_6$  acetonitrile solution at a scan rate of 100 mV/s at room temperature (vs an Ag quasi-reference electrode).

Figure III-17. Cyclic voltammetry curves of YJ-67, YJ-68 in 0.1 M  $\text{Bu}_4\text{NPF}_6$  acetonitrile solution at a scan rate of 100 mV/s at room temperature

(vs an Ag quasi-reference electrode).

Figure III-18. Cyclic voltammetry curves of YJ-69 and YJ-70 in 0.1 M  $\text{Bu}_4\text{NPF}_6$  acetonitrile solution at a scan rate of 100 mV/s at room temperature (vs an Ag quasi-reference electrode).

Figure III-19. Cyclic voltammetry curves of YJ-71, YJ-72, YJ-73 and YJ-74 in 0.1 M  $\text{Bu}_4\text{NPF}_6$  acetonitrile solution at a scan rate of 100 mV/s at room temperature (vs an Ag quasi-reference electrode).

Figure III-20. J-V curves of the solar cell devices based on YJ-61, YJ-62 under  $100\text{mW} / \text{cm}^2$  AM 1.5G illumination.

Figure III-21. J-V curves of the solar cell devices based on YJ-63 ~ YJ-68 under  $100\text{mW} / \text{cm}^2$  AM 1.5G illumination.

Figure III-22. J-V curves of the solar cell devices based on YJ-69, YJ-70 under  $100\text{mW} / \text{cm}^2$  AM 1.5G illumination.

Figure III-23. J-V curves of the solar cell devices based on YJ-71 ~ YJ-74 under  $100\text{mW} / \text{cm}^2$  AM 1.5G illumination.

## List of Tables

Table III-1. Polymerization Results.

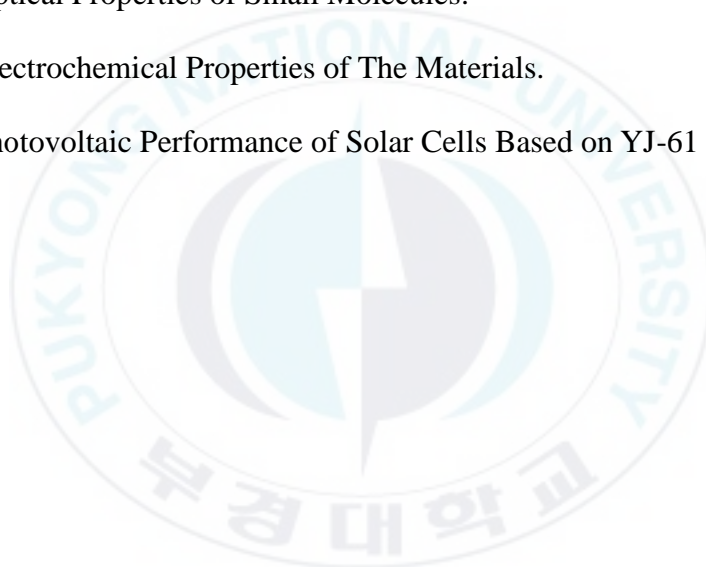
Table III-2. Decomposition Temperatures of Materials.

Table III-3. Optical Properties of Polymers.

Table III-4. Optical Properties of Small Molecules.

Table III-5. Electrochemical Properties of The Materials.

Table III-6. Photovoltaic Performance of Solar Cells Based on YJ-61 ~ YJ-74.



## List of Schemes

- Scheme 1. Synthetic route of donor monomers. (BDT derivatives).
- Scheme 2. Synthetic route of difluoroquinoxaline (T, bi-T and TT).
- Scheme 3. Synthetic route of donor monomer (3T)
- Scheme 4. Synthetic route of donor monomer (stannyl thiophene derivatives)
- Scheme 5. Synthetic route of didodecyldifluoroquinoxaline (DFQ<sub>x</sub>).
- Scheme 6. Synthetic route of didohexcyldifluoroquinoxaline (DFQ<sub>x</sub>).
- Scheme 7. Synthetic route of mono-Br or di-Br dithienoquinoxaline(DTDFQ<sub>x</sub>).
- Scheme 8. Synthetic route of PbiTz-DFQ<sub>x</sub> (YJ-61).
- Scheme 9. Synthetic route of PbiTz-DTDFQ<sub>x</sub> (YJ-62).
- Scheme 10. Synthetic route of 2TQ<sub>x</sub> (YJ-63).
- Scheme 11. Synthetic route of TTQ<sub>x</sub> (YJ-64).
- Scheme 12. Synthetic route of 3TDFQ<sub>x</sub> (In) (YJ-65).
- Scheme 13. Synthetic route of 3TDFQ<sub>x</sub> (Out) (YJ-66).
- Scheme 14. Synthetic route of T-TT-DFQ<sub>x</sub> (In) (YJ-67).
- Scheme 15. Synthetic route of T-TT-DFQ<sub>x</sub> (Out) (YJ-68).

Scheme 16. Synthetic route of biT(DTDFQx)<sub>2</sub> (YJ-69).

Scheme 17. Synthetic route of TT(DTDFQx)<sub>2</sub> (YJ-70).

Scheme 18. Synthetic route of EH-BDT(DTDFDDoQx)<sub>2</sub> (YJ-71).

Scheme 19. Synthetic route of EH-BDT(DTDFDHexQx)<sub>2</sub> (YJ-72).

Scheme 20. Synthetic route of Oct-BDT(DTDFDDoQx)<sub>2</sub> (YJ-73).

Scheme 20. Synthetic route of Oct-BDT(DTDFDHexQx)<sub>2</sub> (YJ-74).



# OPV 를 위한 Quinoxaline 을 기반으로 한 새로운 타입의 A-A 교대구조를 가지는 공액중합체와 단분자들의 합성과 특성

공민성

부경대학교 대학원 공업화학과

요 약

최근 2050년경 천연자원이 고갈 될 것이라는 주장이 점쳐지고 있으며, 이는 환경오염의 문제와 맞물려 친환경 재생에너지의 개발을 필요로 하고 있는 추세이다. 이러한 친환경, 재생 가능한 에너지의 종류로는 수력, 풍력, 지력, biomass 그리고 태양 에너지 등이 있으며, 이중 태양을 이용한 에너지는 무한한 에너지를 가지고 있고, 전 세계 어느 나라에서든 용이한 접근성의 두 가지 장점을 가지고 있어 많은 연구가 활발히 진행되고 있다. 기존에 사용하던 실리콘과 같은 무기물질을 사용한 태양전지는 그 재료비용과 제작비용이 비싸다는 단점을 가지고 있어 경제적, 시장적 가치가 많이 떨어지고 있다. 이러한 단점을 극복하고자 가격이 저렴한 태양전지가 요구되고 있으며, 그 중 전도성의 성질을 띤 고분자, 저분자를 이용한 유기태양전지는 role-to-role 공정, 용액공정을 통한 대면적 생산의 용이성 때문에 그 제작 비용이 크게 절감되고 잘 휘어지는 유연한 물성을 동시에 지니고 있어 다양한 분야에 적용 가능하다는 장점을 가지고 있어 최근 많은 연구가 진행되고 있다. 이 연구에서는 electron-withdrawing 물질로 fluorine이 치환된 Quinoxaline을 사용하여 공액고분자 및 저분자 물질들을 합성하고 그 특성들을 분석 하였다. 고분자로서는 Bithiazole unit과 결합 되었을 때, 저분자에서는 electron-donating 물질로 Benzodithiophene unit과 결합하여 alkyl group이 바뀌었을 때, 또 electron-donating 물질로 thiophene을 도입하였을 때 그 개수, bi-thiophene, fused-thiophene, 그리고 sidechain의 배열이 바뀌었을때, 각각 device를 만들었을 때 효율에 어떠한 영향이 작용하는지에 대해 연구를 실시하였다.

## **Chapter I. Introduction**

### **I-1. The Background of Polymer Solar Cells (PSCs) and Small Molecule Solar Cells (SMSCs)**

Recently, as the rapid development of the world have been in progress, energy demands and consumptions are growing sharply. Furthermore, many researchers are forecasting that natural resources like natural oil and gas, coal will be exhausted in about 2050 years. In accordance with that, many kinds of renewable energies such as geothermal, wind, water, hydrogen, bioenergy and solar energy have been developed by outstanding researchers, scientists in advanced countries. Among these novel energies, solar energy is getting the limelight and growing steadily because of the many merits including infinite energy and non-pollution. In many sorts of energy using solar, inorganic photovoltaic technology based on inorganic materials, especially silicon was used to best way to obtain the high power conversion efficiency (PCE), before. But, nowadays, this way have shown the limitation because of not affordable material and manufacturing costs. To overcome this problems, polymer solar cells (PSCs), small molecule solar cells (SMSCs) based on conjugated materials have drawn attraction in the world. First, polymer solar cells (PSCs) have been attracted notice of the world due to the advantages, such as light weight, flexibility, large area and affordable cost

according to the solution process.<sup>1-3</sup> Another important merit of it is the variety of the polymer structure, which can adjust the backbone and sidechain as occasion demands. By using these crucial advantages, recently, power conversion efficiency (PCE) of photovoltaics are reported over 10%.<sup>4-7</sup> Secondly, small molecule solar cells (SMSCs) have same advantages of the polymer solar cell (PSCs). in addition to that, SMSCs have the high reproducibility.<sup>8-9</sup> Compared to the PSCs, SMSCs have similar optical, photovoltaic properties and parameters when target materials (polymer, small molecule) was synthesized and measured. Because of these reproducibility, recently, study and research related with SMSCs have been currently underway. These device based on SMSCs have shown high PCE keeping up with PSCs over 8~9%.<sup>10-11</sup> To success to commercialize these technologies despite of advantages and high PCE, it is necessary to stability of device, long life time and corresponding to 20% PCE value.

## I-2. Operating Mechanism of Photovoltaic device

As shown in Figure I-1, general operating principle in acceptor-donor type solar cells has four stage. First of all, photoexcitation and exciton generation is occurred, when the absorption of light energy reach active layer. Secondly, exciton diffusion is happen. The excitons pass through donor-acceptor (D-A) interface. At this time, if exciton diffusion is going well, exciton diffusion length will within around 10 nm. Next stage is electron-hole pairs (exciton) was dissociated with electrons, which is forward acceptor area, and holes that forward donor area, respectively. And then charge transport and collection is ongoing with separated holes and electrons passing through anode and cathode, respectively.

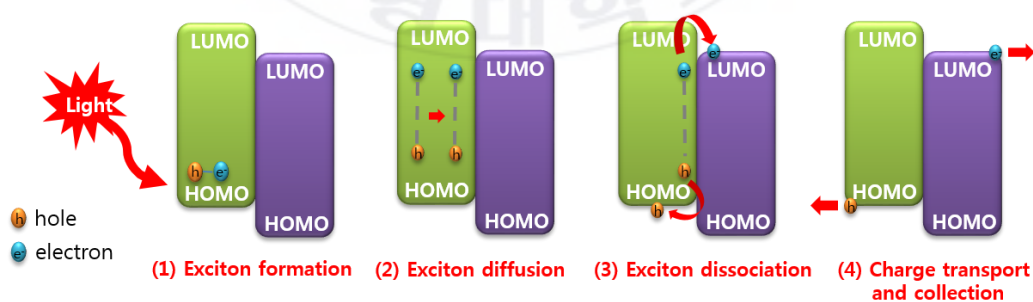


**Figure I-1.** Working mechanism of donor-acceptor type heterojunction solar cells.

### I-3. Bulk Heterojunction Structure

Before using the bulk heterojunction (BHJ) type solar cells, which have mixed phase with donor (conjugated polymer/monomer) and acceptor (conjugated polymer/monomer, fullerene derivatives), bilayer type was used to photovoltaic device. These conventional devices consist of sequentially arranged with n-type and p-type material, separately, have limited charge separation and generate exciton recombination because of small interfacial area and long exciton diffusion length ( over 20 nm). It bring on the loss of photons and lead to low quantum efficiencies.<sup>12</sup> Compared to bilayer, The BHJ type solar cells have blended n-type and p-type as mentioned. So it could widen the interfacial area between the donor and acceptor and narrow the exciton diffusion length (~10 nm). Therefore, according to the operating principle (Figure I-1), exciton diffusion could be going well and charge recombination be less generated than bilayer. As a result of that, charge carrier mobility is better and more photons is generated, it lead to better  $J_{sc}$ . The other important fact of BHJ type solar cells is morphology. It is important how well domain is created heterogeneously, and domain size is narrowed (~10 nm). Satisfaction of these essential two keys result in better crystallites, charge transfer, more photons and  $J_{sc}$ .<sup>13-17</sup>

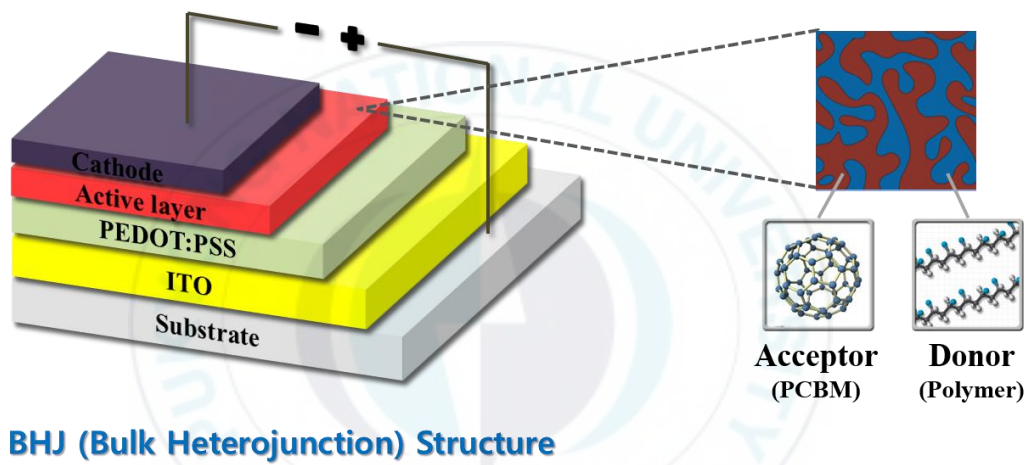


**Figure I-2.** Structures of bulk-heterojunction device.

## **I-4. Parameters of PSCs**

To achieve better PCE ( $=V_{oc} \times J_{sc} \times FF / P_{in}$ ) value, the three factors in the bracket is important and need to be carefully handled. Each important parameters is introduced under in detail.

### **I-4-1. Open-Circuit Voltage ( $V_{oc}$ )**

The open-circuit voltage ( $V_{oc}$ ) means that the maximum voltage when current value is zero, that is disconnection of any circuits. This factor is thoroughly involved in the difference between the highest occupied molecular orbital (HOMO) level of the donor materials and the lowest unoccupied molecular orbital (LUMO) level of the acceptor materials.<sup>18</sup> In order to achieve higher  $V_{oc}$ , Using donor material with deep HOMO levels is essential, however, the donor material having very low HOMO levels cause negative impact on performance of PSCs and SMSCs. This is because threshold 0.3 eV of minimum energy difference between the LUMO energy level of the donor material and the acceptor is required for effective charge transfer, but using material with very deep HOMO levels not satisfy this condition. Also, lowering the HOMO level of the donor material have another negative effect. It causes widening bandgap of donor material and it could decrease the light absorption ability of the donor

material and it results in low  $J_{sc}$ . When considering these two point of view, designing and synthesizing the donor material with appropriate energy level and low band gap are required for outstanding performance of the PSCs.<sup>19,20</sup>

#### **I-4-2. Short-Circuit Current Density ( $J_{sc}$ )**

The short-circuit current density ( $J_{sc}$ ) is the current passing through the photovoltaic device when the effective voltage taken through the device is zero. The  $J_{sc}$  intimately linked with the number of the excitons created for a period of solar irradiation. In order to maximize the exciton generation, the absorption ability of the active layer in device have to be matched with the spectrum of the sun light. In the old days, because only PCBM derivatives was used as acceptor material, which has poor absorption in the visible and near-IR area where about 70% of the solar flux is compacted.<sup>21</sup> Adjustment of light absorption ability of the donor material was necessary for the higher  $J_{sc}$ . But, nowadays, some kinds of different type solar cell (all polymer solar cell, small molecule used as acceptor like ITIC) have been developed. On the contrary, acceptors of these type solar cells absorb a long wavelength range 300 ~ 900 nm.<sup>22,23</sup> Another important factor in generating excitons is bandgap, which have to be adjusted from 1.4 to 1.5 eV. Even if the narrow band gap is essential for the device to enhance light absorption and exciton generation, too low band gap take a negative effect that HOMO level of the donor materials more high and it lead to reduce the  $V_{oc}$ . To sum it all up, in an attempt to obtain the excellent  $J_{sc}$ , donor material have to be designed have a

good absorption in range visible and IR region, especially 300 ~ 900nm, and suitable band gap between 1.4 and 1.5 eV. In addition, because there are many other factor influencing  $J_{sc}$  values such as charge transfer, molecular weight and morphology of device, many research are necessary.

### **I-4-3. Fill Factor (FF)**

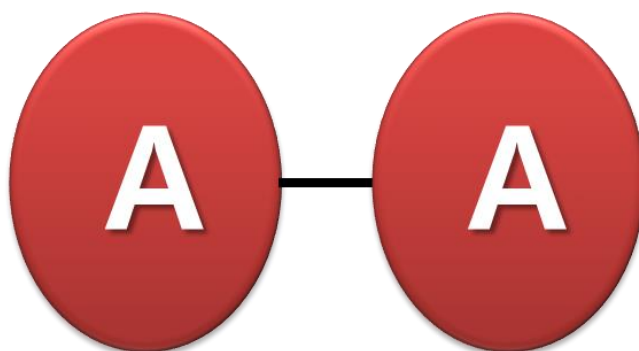
Fill factor (FF) is the ratio between the maximum obtainable power and the product of  $J_{sc}$  and  $V_{oc}$ . FF have a close connections with many factors such as film morphology, charge carrier mobility, blending ability between donor and acceptor. But, among these factor, an accurate connection is undisclosed.<sup>24</sup> In order to achieve better FF, some modification of side-chain and planarity of molecule are necessary by controlling materials. First, side-chain influence on intermolecular interaction, solubility and crystallinity due to the steric hindrance and packing ability of material. Therefore, suitable side-chain is critical for the excellent figure by optimizing  $\pi$ -  $\pi$  stacking and crystallinity. Secondly, planarity of backbone also influence on the figure. More increasing the planarity, more decreased space between intermolecular and it lead to more intermolecular interaction with directivity in out of plane. And then  $\pi$ -  $\pi$  stacking is increased. However, because FF is related with other variables, more consideration and design is necessary.

## **I-5. Methods to Synthesize Conjugated Materials for High Performance.**

### **I-5-1. Acceptor-Acceptor (A-A) Type Polymer**

In the past days, donor-acceptor type conjugated materials have been used as active materials for organic electronic devices such as OLED, photovoltaics and OFET.<sup>25,26</sup> But, so far, there are not many research studies on A-A type polymers as p-type materials. And then, our lab have studied for A-A type polymer solar cells as p-type materials.

There are two advantages of using A-A type materials. First of all, It has good air stability.<sup>27</sup> Air stability is essential for polymer solar cells, because photovoltaic devices must be exposed air condition. Secondly, it has good merit of strong absorption for light.<sup>28</sup> Strong absorption for near IR will results in good EQE spectra, which leads to more generation of photocurrent. Finally, more high value of  $J_{sc}$  would be measured.



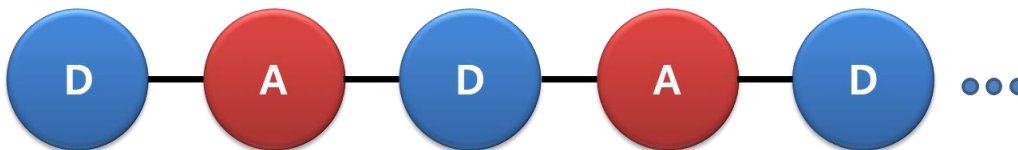
- Composed of two electron-deficient unit (**Acceptor**)- (**Acceptor**)
- Air condition stability
- Increase of light absorption

**Figure I-3.** Acceptor-acceptor type polymer solar cells

### **I-5-2. Small Molecule**

In contrast with polymer materials, small molecules have the merits of molecular weights and well-investigated structures. Small molecules are also have simple purification process, good reproductibility, which will enrich the selection of the materials for commercialization of photovoltaics.<sup>29</sup>

**A Type : Polymer**



**B Type : Small molecule**



**Figure I-4.** Two types of organic solar materials.

### **I-5-3. Influence of Functionalities Substitution in Conjugated Backbone**

Many kinds of properties of organic materials like solubility, crystallinity and absorption and electrochemical energy levels (both HOMO and LUMO energy levels.) can be changed by introduction of functional group, which will effect  $J_{sc}$ ,  $V_{oc}$ , FF and PCE of photovoltaic devices. Among various functional group, fluorine is the smallest unit with very strong electron with-drawing effect (van der Waals radius of 1.35 Å and electronegativity of 4.0)

There are many advantages of using fluorine atoms. First of all, the introduction of fluorine is effective to lower the HOMO energy level, which results in higher

$V_{oc}$ . In comparison with the reduced HOMO energy level, decreased LUMO energy level was lesser. In this reason, the band gap was widened as a result. Although it was happened, the loss by widened bandgap was so small that  $J_{sc}$  seldom affect.

Second, the introduction of fluorine reduced steric hindrance and improved domain purity and crystallinity. Resultingly, FF would be higher due to the generation of good morphology and interaction.

#### **I-5-4. Selection of Donor and Acceptor Unit in Conjugated Materials**

The bithiazole (biTz) is used as a acceptor unit in A-A type PSCs. This unit has broad absorption in infrared region, which will enhance  $J_{sc}$ . And it has two nitrogen of imine group that lead to lower HOMO energy level.

The benzo[1,2-*b*:4,5-*b'*]-dithiophene (BDT) is one of prospective donor material with weaker donating ability, which will lower HOMO level. The BDT unit is consist of benzene ring in the center and two fused flanking thiophene unit in the each arms. These BDT unit have structural advantages such as more planner and rigid backbone result in better  $\pi$ - $\pi$  stacking with inter-molecule and hole mobility, which would improve  $J_{sc}$  and FF.<sup>30-33</sup> As mentioned before, BDT has weaker electron-donating ability. Therefore, the HOMO energies of BDT containing materials are closer to the ideal HOMO levels.<sup>34-37</sup>

The quinoxaline (Qx) unit have used as acceptor unit due to two electron

deficient carbon-nitrogen double bond (C=N) with strong electronegativity. And important merit of Qx is that the maintaining the low-lying HOMO energy level can be for the synthesized materials, which would be advantageous for getting a more high  $V_{oc}$  in the resulting photovoltaic devices. And Qx has possibility of alkylation compared to benzothiadiazole (BT). Therefore, the Qx unit could insert the alkyl chain to fortify solubility on the main backbone without causing steric hinderance.<sup>38-39</sup>



## Chapter II. Experimental

### II-1. Materials and Instruments

The monomer, 4,4'-dibutoxy-2,2'-bis(trimethylstannyl)-5,5'-bithiazole (98%), was purchased from Suna Tech Inc. and used as received. The other reagents were purchased from Acros, Aldrich, Alfa or TCI, and used without further purification. Solvents were distilled with sodium from refinement equipment and handled under moisture-free atmosphere.  $^1\text{H}$  and  $^{13}\text{C}$  NMR spectra were recorded with a JEOL JNM ECP-400 spectrometer and chemical shifts were recorded in part per million (ppm) units with TMS as the internal standard. Flash column chromatography was performed with Merck silica gel 60 (particle size; 230 - 400 mesh ASTM) with ethyl acetate / hexane / methylene chloride gradients unless otherwise indicated. Analytical thin layer chromatography (TLC) was conducted using Merck 0.25 mm silica gel 60F pre-coated aluminum plates with fluorescent indicator UV254. High resolution mass spectra (HRMS) were recorded on a JEOL JMS-700 mass spectrometer under electron impact (EI) or fast atom bombardment (FAB) conditions. Elemental analyses (EA) were performed by Flash EA 1112 Series. The UV-vis absorption spectra were recorded by a Varian 5E UV/VIS/NIR spectrophotometer. The CV was performed with a solution of

tetrabutylammonium hexafluorophosphate ( $\text{Bu}_4\text{NPF}_6$ ; 0.10 M) in acetonitrile at a scan rate of 100 mV/s at room temperature. Pt wire and Ag/AgNO<sub>3</sub> electrode were used as the counter electrode and reference electrode, respectively. The energy level of the Ag/AgNO<sub>3</sub> reference electrode (calibrated by the FC/FC<sup>+</sup> redox system) was 4.80 eV below the vacuum level. HOMO levels were calculated according to the empirical formula ( $E_{\text{HOMO}} = -([E_{\text{onset}}]_{\text{ox}} + 4.80)$  eV). For the EL experiment, poly(3,4-ethylenedioxythiophene) (PEDOT) doped with poly(styrenesulfonate) (PSS), as the hole-injection-transport layer, was introduced between emissive layer and ITO glass substrate cleaned by successive ultrasonic treatments. The solution of the PEDOT:PSS in aqueous isopropyl alcohol was spin-coated on the surface-treated ITO substrate and dried on a hot plate for 30 min at 110 °C. On top of the PEDOT:PSS layer, the film of photoactive layer was obtained by spin casting *o*-dichlorobenzene solution blended with polymer and PCBM. The film was dried in vacuum, and aluminum electrodes were deposited on the top of the small molecule films through a mask by vacuum evaporation at pressures below 10<sup>-7</sup> torr, yielding active areas of 4 mm<sup>2</sup>.

## II-2. Synthesis of Monomers

### II-2-1. Synthesis of Donor Monomers

#### II-2-1-1. Synthesis of thiophene-3-carbonyl chloride (2)

Thiophene-3-carboxylic acid (10 g, 78.03 mmol) and 100 mL of methylene chloride were put into a 250 mL flask. The mixture was cooled by ice-water bath, and then oxalyl chloride (78.03 g, 156.07 mmol) was added in one portion. The reactant was stirred overnight at ambient temperature, and a clear solution was obtained. After removing the solvent and unreacted oxalyl chloride by rotary evaporation, compound **2** was obtained as white solid. It was dissolved into 100 mL of methylene chloride and used for the next step.

#### II-2-1-2. Synthesis of *N,N*-diethylthiophene-3-carboxamide (3)

In a 250 mL flask in ice-water bath, 16.15 mL of diethylamine (156.07 mmol) and 100 mL of methylene chloride were mixed, and the solution of thiophene-3-carbonyl chloride was added into the flask slowly. After all of the solution was added, the ice bath was removed, and the reactant was stirred at ambient temperature for 30 min. Then, the reactant was washed by water several times, and the organic layer was dried over anhydrous  $\text{MgSO}_4$ . After removing solvent,

the crude product was purified by flash chromatography (EtOAc/hexane, 1:4) to give 12 g (91%) of compound **3** as pale yellow oil ;  $^1\text{H}$  NMR (300 MHz,  $\text{CDCl}_3$ ):  $\delta$  7.46 (d, 1H,  $J = 1.09$  Hz), 7.30 (t, 1H,  $J = 1.09$  and 4.94 Hz), 7.17 (d, 1H,  $J = 4.94$  Hz), 1.18 (m, 10H);  $^{13}\text{C}$  NMR (75 MHz,  $\text{CDCl}_3$ )  $\delta$  166.64, 137.53, 13.08, 125.88, 43.32, 14.59, 39.81 HRMS( $\text{EI}^+$ ,  $m/z$ ) [ $\text{M}$ ] $^+$  calcd for  $\text{C}_9\text{H}_{13}\text{NOS}$  183.0718, measured 183.0717.

### II-2-1-3. Synthesis of benzo[1,2-*b*:4,5-*b'*]dithiophene-4,8-dione (**4**)

Compound **3** (70.93 mmol, 12 g) was put into a well-dried flask with 25 mL of THF under an inert atmosphere. The solution was cooled down by an ice-water bath, and 32 mL of *n*-butyllithium (85.12 mmol, 2.5 mol/L) was added into the flask dropwise within 30 min. Then, the reactant was stirred at ambient temperature for 2 hr. The reactant was poured into ice water and stirred for several hours. The mixture was filtrated, and the yellow precipitate was washed by 100 mL of water, 50 mL of methanol, and 50 mL of hexane successively. 7.5 g of compound **4** was obtained as a yellow powder (34.04 mmol, yield 96%). Mp 241 °C ;  $^1\text{H}$  NMR (300 MHz,  $\text{CDCl}_3$ ):  $\delta$  7.15 (d, 2H,  $J = 4.94$  Hz), 6.46 (d, 2H,  $J = 5.22$  Hz) ;  $^{13}\text{C}$  NMR (75 MHz,  $\text{CDCl}_3$ )  $\delta$  174.69, 145.14, 143.06, 133.78, 126.81 HRMS( $\text{EI}^+$ ,  $m/z$ ) [ $\text{M}$ ] $^+$  calcd for  $\text{C}_{10}\text{H}_4\text{O}_2\text{S}_2$  219.9653, measured 219.9652.

#### **II-2-1-4. Synthesis of 4,8-bis(2-ethylhexyloxy)benzo[1,2-*b*:4,5-*b'*]dithiophene (5)**

To a mixture of compound **4** (4 g, 18 mmol) and zinc powder (2.6 g, 40 mmol) was added 5 N NaOH aqueous solution (37 mL) and the mixture was stirred under reflux for 3 hr. After 2-ethylhexyl bromide (22.26 g, 54 mmol) and tetrabutylammoniumbromide (0.9 g, 3.64 mmol) were added to the mixture, the reaction mixture was further refluxed for 12 hr. The reaction mixture was then extracted with diethyl ether, and the organic layer was washed with brine and dried over anhydrous MgSO<sub>4</sub>. After evaporating the solvent, the crude product was purified by silica gel chromatography using hexane to yield as a light yellow oil, yield 55%. <sup>1</sup>H NMR (CDCl<sub>3</sub>, 400 MHz, δ): 7.48(d, 2H, J = 5 Hz), 7.46 (d, 2H, J = 5 Hz), 4.18 (br, 4H), 1.78 (m, 2H), 1.73–1.25 (m, 16H), 0.92–1.03 (t, 12H, J = 7 Hz).

#### **II-2-1-5. Synthesis of 2,6-bis(trimethyltin)-4,8-bis(2-ethylhexyloxy)benzo[1,2-*b*:3,4-*b'*]dithiophene (6)**

To a solution of compound **5** (4 g, 5.1 mmol) in anhydrous THF (35 mL) was added dropwise *n*-butyllithium (2.5 M in hexane, 8.16 mL, 20.4 mmol) via syringe at -78 °C under nitrogen atmosphere. The mixture was stirred at -78 °C for 30 min and then at room temperature for 30 min. After the mixture was cooled to -78 °C again, trimethyltin chloride (25.5 g, 25.5 mmol) was added. The

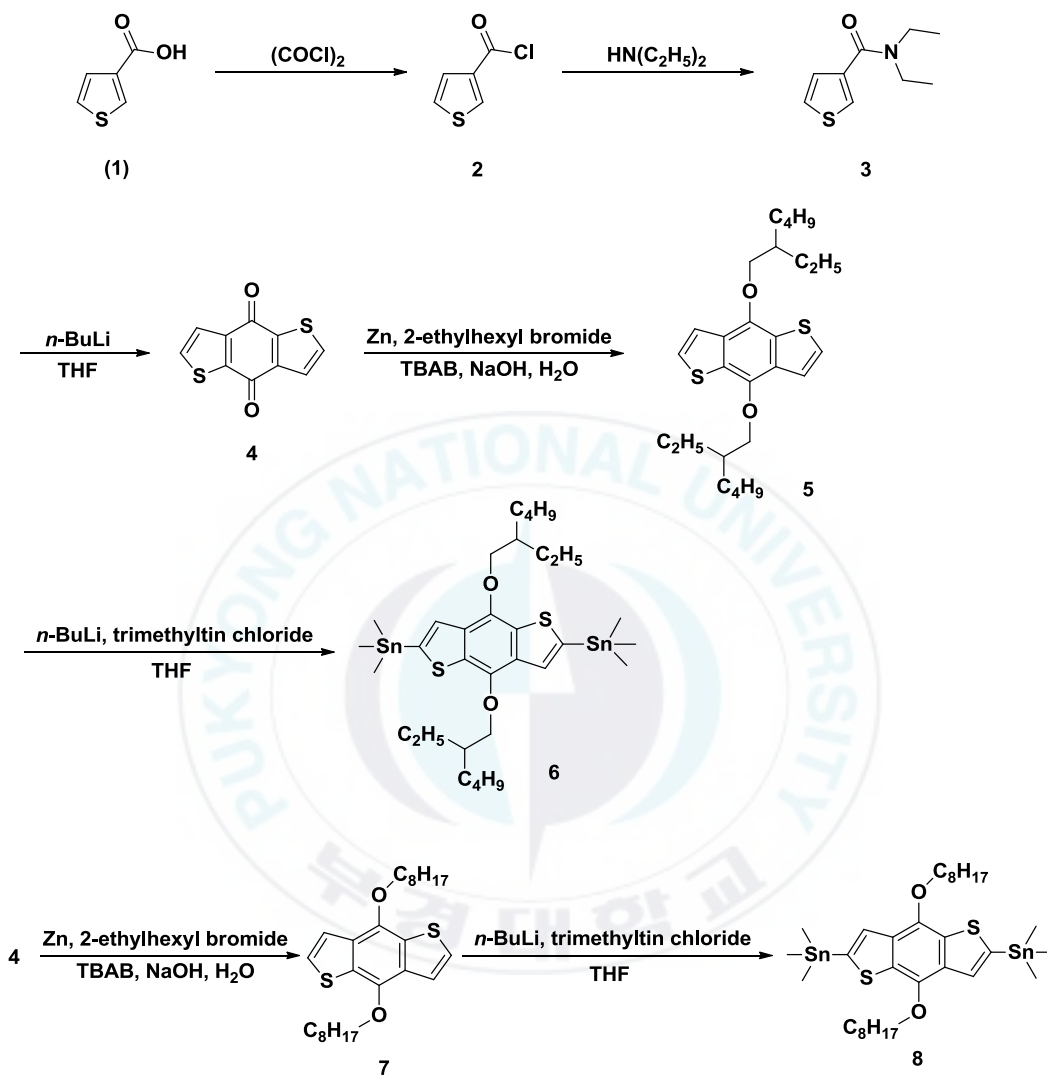
mixture was warmed to room temperature and stirred for 12 hr. After quenching the reaction with water, the volatile species were evaporated in vacuo. The residue was extracted with hexane, and the organic layer was washed with brine, dried over anhydrous MgSO<sub>4</sub>, and concentrated. The crude product was purified by recrystallization from methanol to yield as a colorless needles (5 g, 4.51 mmol, 88%). M.p. 60-61 °C. <sup>1</sup>H NMR (CDCl<sub>3</sub>, 400 MHz, δ): 7.50 (t, 2H, J = 14.64 Hz), 4.17 (d, 4H, J = 5.36 Hz), 1.80 (m, 2H), 1.32-1.72 (m, 16H), 1.01 (t, 6H, J = 7.38 Hz), 0.93 (t, 6H, J = 7.12 Hz), 0.43 (m, 18H)

#### **II-2-1-6. Synthesis of 4,8-bis(octyloxy)benzo[1,2-b:4,5-b']dithiophene (7)**

To a mixture of compound 4 (4 g, 18 mmol) and zinc powder (2.6 g, 40 mmol) was added 5N NaOH aqueous solution (37 mL) and the mixture was stirred under reflux for 3 hr, After octyl bromide (22.26 g, 54 mmol) and tetrabutylammoniumbromide (0.9 g, 3.64 mmol) were added to the mixture, the reaction mixture was further refluxed for 12 hr. The reaction mixture was then extracted with diethyl ether, and the organic layer was washed with brine and dried over anhydrous MgSO<sub>4</sub>. After evaporating the solvent, the crude product was purified by silica gel chromatography using hexane to yield as a light yellow oil, yield 55%. <sup>1</sup>H NMR (CDCl<sub>3</sub>, 400 MHz, δ):

### II-2-1-7. Synthesis of 2,6-bis(trimethyltin)-4,8-bis(octyloxy)benzo[1,2-*b*:3,4-*b'*]dithiophene (8)

To a solution of compound **7** (4 g, 5.1 mmol) in anhydrous THF (35 mL) was added dropwise *n*-butyllithium (2.5 M in hexane, 8.16 mL, 20.4 mmol) via syringe at -78 °C under nitrogen atmosphere. The mixture was stirred at -78 °C for 30 min and then at room temperature for 30 min. After the mixture was cooled to -78 °C again, trimethyltin chloride (25.5 g, 25.5 mmol) was added. The mixture was warmed to room temperature and stirred for 12 hr. After quenching the reaction with water, the volatile species were evaporated in vacuo. The residue was extracted with hexane, and the organic layer was washed with brine, dried over anhydrous MgSO<sub>4</sub>, and concentrated. The crude product was purified by recrystallization from methanol to yield as a colorless needles (4.98 g, 4.51 mmol, 88%). M.p. 60-61 °C. <sup>1</sup>H NMR (CDCl<sub>3</sub>, 400 MHz, δ): 7.50 (t, 2H, J = 14.64 Hz), 4.17 (d, 4H, J = 5.36 Hz), 1.80 (m, 2H), 1.32-1.72 (m, 16H), 1.01 (t, 6H, J = 7.38 Hz), 0.93 (t, 6H, J = 7.12 Hz), 0.43 (m, 18H)



**Scheme 1.** Synthetic route of donor monomers (BDT derivatives).

#### II-2-1-8. Synthesis of 2,5-bis(trimethylstannyl)thiophene (10)

To a solution of 1 g (11.88 mmol) of thiophene in 40 mL of THF at -78 °C under argon was slowly added 27.95 mL (47.52 mmol) of 1.7 M *t*-Butyllithium in THF. After 30 min at -78 °C, the reaction mixture was warmed to room temperature, stirred for 1 hr and cooled back to -78°C. The reaction mixture was added 49.9 mL (49.9 mmol) of 1M trimethyltin chloride. After 30 min at -78°C, the reaction mixture was warmed to room temperature, stirred for overnight, treated with 20 ml of water. The reaction mixture was diluted with ether and washed with water. The combined organic phase was dried MgSO<sub>4</sub> after removal of the solvent under reduced pressure. The crude brown solid was recrystallized from ether/EtOH to give 1.02 g (28%) of compound white solid. <sup>1</sup>H NMR (CDCl<sub>3</sub>, 300MHz, δ): 7.37 (s, 2H), 0.34 (s, 18H). <sup>13</sup>C NMR (75 MHz, CDCl<sub>3</sub>) δ 205.39, 136.00, -9.02. HRMS (FAB<sup>+</sup>, m/z) [M]<sup>+</sup> calcd for C<sub>10</sub>H<sub>20</sub>SSn<sub>2</sub> 411.9330, measured 411.9335.

#### II-2-1-9. Synthesis of 5,5'-bis(trimethylstannyl)-2,2'-bithiophene (12)

A solution of n-butyllithium (6.34 mL, 15.84 mmol, 2.5 M in hexane) was added slowly to 2,2'-bithiophene (3 g, 18.04 mmol) in tetrahydrofuran (100 mL) at -78 °C. After addition, the mixture was stirred for 30 min at -78 °C, then warmed to 0 °C and stirred for 30 min. The mixture was cool to -78 °C again. Trimethyltin chloride solution (15.84 mL, 15.84 mmol, 1.0 M in hexane) was added to the

mixture. The mixture was warmed to room temperature and stirred overnight. The reaction was quenched with addition of water (150 mL) and was extracted with diethyl ether for three times. The combined organic layer was dried with anhydrous sodium sulfate. Solvent was removed under reduced pressure and residue was purified by recrystallization in ethanol to afford a grey solid (5.94 g, 66.94%).  $^1\text{H}$  NMR (DMSO- $d_6$ , 400 MHz,  $\delta$ ): 7.33 (2H, d), 7.13 (2H, d), 0.35 (18H, s).

#### **II-2-1-10. Synthesis of 2,5-Bis-trimethylstannyl-thieno[3,2-*b*]thiophene (14)**

A solution of *n*-butyllithium (9.41 mL, 23.53 mmol, 2.5 M in hexane) was added slowly to thieno[3,2-*b*]thiophene (1.50 g, 10.70 mmol) in tetrahydrofuran (50 mL) at -78 °C. After addition, the mixture was stirred for 30 min at -78 °C, then warmed to 0 °C and stirred for 30 min. The mixture was cool to -78 °C again. Trimethyltin chloride solution (23.53 mL, 23.53 mmol, 1.0 M in hexane) was added to the mixture. The mixture was warmed to room temperature and stirred overnight. The reaction was quenched with addition of water (150 mL) and was extracted with diethyl ether for three times. The combined organic layer was dried with anhydrous sodium sulfate. Solvent was removed under reduced pressure and residue was purified by recrystallization in ethanol to afford a white solid (3.10g, 58.73%).  $^1\text{H}$  NMR (DMSO- $d_6$ , 400 MHz,  $\delta$ ): 7.40 (2H, s), 0.35 (18H, s).

### II-2-1-11. Synthesis of 2,5-Dibromothiophene (15)

A solution of *n*-bromosuccinimide (NBS) (8.46 g, 47.54 mmol) in anhydrous DMF (60 mL) was slowly added dropwise in the dark to a solution of thiophene (2 g, 23.77 mmol) in anhydrous DMF (60 mL) at 0 °C. And the mixture was initially stirred at room temperature for 0.5 hr and then at 60 °C for an additional overnight. The reaction was quenched with addition of water (150 mL) and was extracted with diethyl ether for three times. The combined organic phases were dried over anhydrous MgSO<sub>4</sub>. Further purification was run by silica column with petroleum hexane to give an oily liquid. Yield: 5.21g (90.60%). <sup>1</sup>H NMR (CDCl<sub>3</sub>, 300 MHz, δ): 6.84 (s, 2H).

### II-2-1-12. Synthesis of tributyl(thiophen-2-yl)stannane(16)

To a round bottom flask loaded with dry THF (30 mL), thiophene (5 ml, 63.57 mmol) was added and the mixture was cooled to -78 °C by acetone/dry ice bath. *n*-BuLi in hexane solution (1.6 M, 26 mL) was added dropwise. After stirring at -78 °C for 1 hr, tributyl tin chloride (12 ml, 42 mmol) was added dropwise and removed the dry ice bath immediately. After six more hours, the reaction was then terminated by adding saturated NaHCO<sub>3</sub> solution (100 ml) into the flask. The solvent was removed by rotary evaporation. The remaining oil was diluted with diethyl ether and washed with brine several times. The collected organic layer was dried over MgSO<sub>4</sub> and the organic solvent was removed by rotary

evaporation. The collected orange oil was dried under vacuum for another 3 h and used directly for the next step.

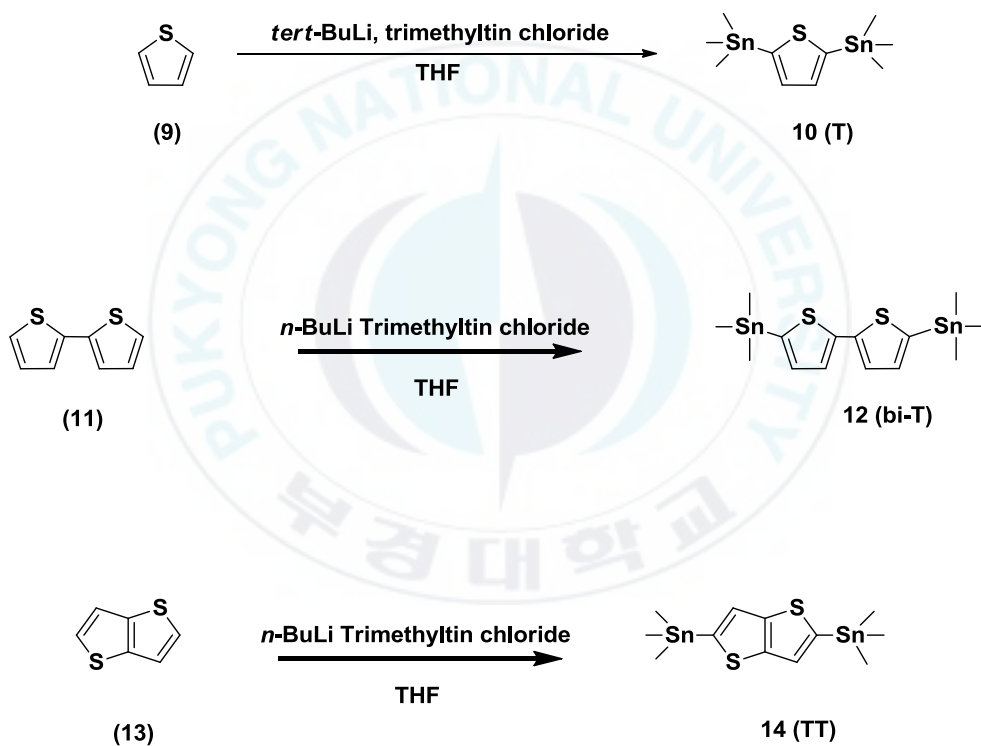
#### **II-2-1-13. Synthesis of 2,2':5',2''-terthiophene (17)**

The solution of 2,5-dibromothiophene (2.94 g, 12.15 mmol), 2-(tributylstannyl) thiophene (9.04 g, 24.22 mmol) and tetrakis(triphenylphosphine)palladium(0) was dissolved in dimethylformamide (30 ml). The mixture was stirred at 80 °C for overnight under argon atmosphere. The aqueous layers were extracted with diethylether, the combined extracts were washed with distilled water, dried over anhydrous MgSO<sub>4</sub>. The solvent was removed by rotary evaporation. Recrystallization of the crude product in ethanol. Yellow solid (yield : 1.72 g, 57.13%). <sup>1</sup>H NMR (CDCl<sub>3</sub>, 300 MHz, δ): 7.20 (dd, 2H), 7.15 (dd, 2H), 7.06 (s, 1H), 7.00 (dd, 2H).

#### **I-2-1-14. Synthesis of 2,5''-Bis(trimethylsilyl)-5,2',5',2''-terthiophene (18)**

To a solution of 2,5''-dibromo-5,2',5',2''-terthiophene (2 g, 8.05 mmol) was dissolved in anhydrous THF (80 mL). The mixture was cooled to -78 °C and *n*-BuLi (7.08 mL, 2.5 M solution) was added dropwise. After the addition, the mixture was stirred at same temperature for 1 h. A solution of trimethyltin chloride (17.71 ml, 1 M) was added dropwise. After stirred overnight, the mixture

was quenched with water. The aqueous layers were extracted with diethylether, the combined extracts were washed with distilled water, dried over anhydrous  $MgSO_4$ . The solvent was removed by rotary evaporation. Recrystallization of the crude product in ethanol. Yellow solid (yield: 2.60 g, 56.27%).  $^1H$  NMR ( $CDCl_3$ , 300 MHz,  $\delta$ ): 7.39 (d, 2H), 7.21 (s, 2H), 7.16 (d, 2H), 0.36 (s, 1H).



**Scheme 2.** Synthetic route of donor monomer (T, bi-T and TT).



### **II-2-1-15. Synthesis of tributyl(3-hexylthiophen-2-yl)stannane (20)**

Compound **19** (4.5 mL, 22.11 mmol) was dissolved in dry THF (60 mL) under nitrogen atmosphere and *n*-BuLi in hexane solution (1.6 M, 9.21 mL) was added at -78 °C. After stirring at -78 °C for 1 hr, tributyl tin chloride (4.14 mL, 14.76 mmol) was added dropwise and removed the dry ice bath and stirred for 24 hr at room temperature. The solvent was removed by rotary evaporation. The remaining oil was diluted with diethyl ether and washed with brine several times. The collected organic layer was dried over MgSO<sub>4</sub> and the organic solvent was removed by rotary evaporation. The collected yellow oil was dried under vacuum for another 3 h and used directly for the next step.

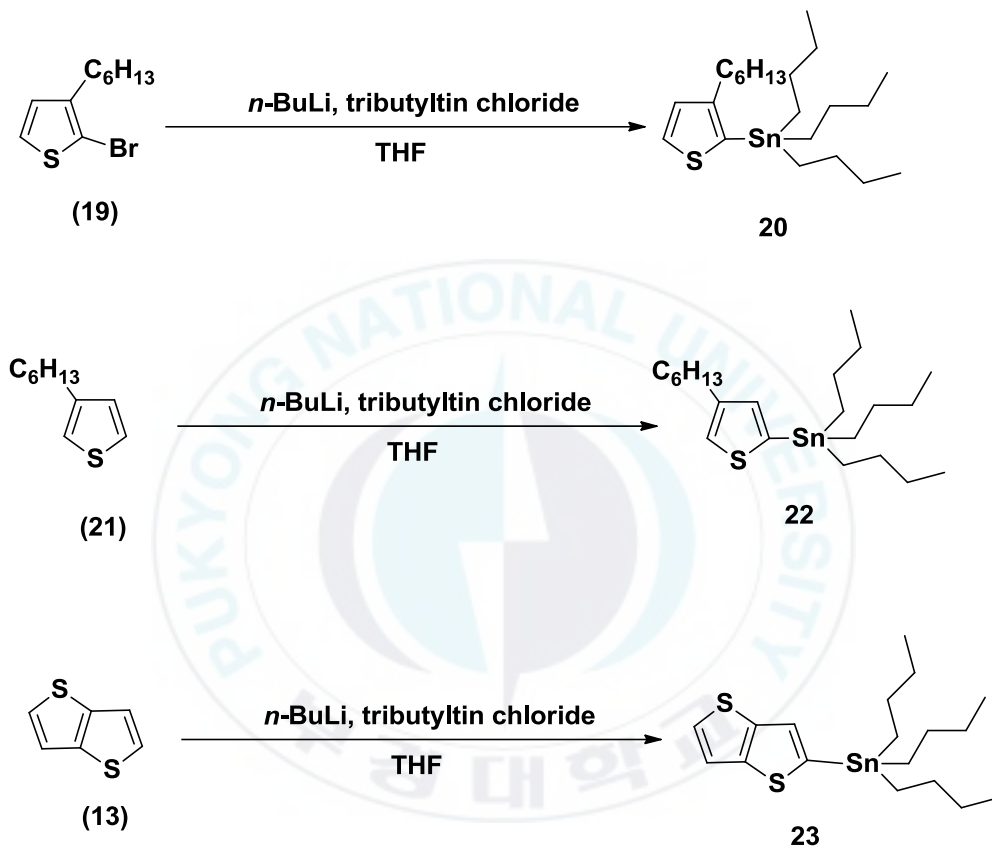
### **II-2-2-16. Synthesis of tributyl(4-hexylthiophen-2-yl)stannane (22)**

Compound **21** (4.5 mL, 25.13 mmol) was dissolved in dry THF (60 mL) under nitrogen atmosphere and *n*-BuLi in hexane solution (1.6 M, 10.47 mL) was added at -78 °C. After stirring at -78 °C for 1 hr, tributyl tin chloride (4.51 mL, 16.76 mmol) was added dropwise and removed the dry ice bath and stirred for 24 hr at room temperature. The solvent was removed by rotary evaporation. The remaining oil was diluted with diethyl ether and washed with brine several times. The collected organic layer was dried over MgSO<sub>4</sub> and the organic solvent was removed by rotary evaporation. The collected yellow oil was dried under vacuum

for another 3 h and used directly for the next step.

### **II-2-1-17. Synthesis of tributyl(thieno[3,2-b]thiophen-2-yl)stanne (23)**

Thienothiophene (1.4 mL, 10.0 mmol) was dissolved in dry THF (20 mL) under argon atmosphere and n-BuLi in hexane solution(2.5M, 10.0mL) was added at -78 °C. After stirring at -78 °C for 1 hr, tributyl tin chloride (3.08 mL, 11.00 mmol) was added dropwise and removed the dry ice bath and stirred for 24 hr at room temperature. The solvent was removed by rotary evaporation. The remaining oil was diluted with diethyl ether and washed with brine several times. The collected organic layer was dried over MgSO<sub>4</sub> and the organic solvent was removed by rotary evaporation. The collected yellow oil was dried under vacuum for another 3 h and used directly for the next step.



**Scheme 4.** Synthetic route of donor monomer (stannyl thiophene derivatives).

## II-2-2. Synthesis of acceptor monomers

### II-2-2-1. Synthesis of 2,3-difluoro-1,4-bis-(trimethylsilyl)benzene (**25**)

*n*-Butyllithium (1.6 M in *n*-hexane, 120 mL, 192 mmol) was added to a solution of di-isopropylamine (27 mL, 192 mmol) in anhydrous THF (80 mL) at -78 °C. After stirring 30 min at -78 °C, 1,2-difluorobenzene (7.5 mL, 77 mmol) and chlorotrimethylsilane (24 mL, 192 mmol) was added to the solution at a rate which allowed the internal reaction temperature to remain below -50 °C. The solution was stirred at -78 °C for an additional 1 hr. 1 M H<sub>2</sub>SO<sub>4</sub> solution (20 mL) was added and then extracted with diethyl ether (20 mL × 3). The combined organic layers were washed with brine, dried over MgSO<sub>4</sub>, and concentrated under reduced pressure to afford colorless needle-shaped crystals of compound **25** (19.0 g, 98%). <sup>1</sup>H NMR (CDCl<sub>3</sub>, 300 MHz, δ): 7.09 (s, 2H), 0.32 (s, 18H). LRMS (EI): *m/z* = 258 (M<sup>+</sup>).

### II-2-2-2. Synthesis of 1,4-dibromo-2,3-difluoro-benzene (**26**)

To a neat bromine (5.3 mL, 103 mmol) cooled to 0 °C was added portion wise solid **25** (8.9 g, 34.4 mmol) while maintaining the internal temperature between 20 and 40 °C. The reaction mixture was stirred at 58 °C for 2 hr. After 1 hr of this period had elapsed, additional bromine (0.9 mL, 17.2 mmol) was added. The reaction mixture was cooled to 0 °C and slowly poured into ice-cold saturated

NaHCO<sub>3</sub> solution and extracted with diethyl ether (50 mL × 3). The combined organic layers were washed with brine, dried over MgSO<sub>4</sub>, and concentrated under reduced pressure to afford colorless liquid of compound **26** (9.2 g, 99%).  
<sup>1</sup>H NMR (CDCl<sub>3</sub>, 300 MHz, δ): 7.23 (m, 2H). LRMS (EI): m/z = 272 (M<sup>+</sup>).

### II-2-2-3. Synthesis of 1,4-dibromo-2,3-difluoro-5,6-dinitro-benzene (**27**)

In a 500 mL flask, concentrated sulphuric acid (44 mL) was added and cooled to 0-5°C in an ice water bath. Fuming nitric acid (44 mL) and 2,3-difluoro-1,4-dibromo-benzene (8.8 g, 32.5 mmol) were slowly added. Then, the flask was heated to 65 °C for 14 hr. The mixture was then precipitated into ice water. The resulting yellow solid was filtered and purified by column with petroleum hexane/CH<sub>2</sub>Cl<sub>2</sub> (4:1) to afford a white solid of compound **27** (3.4 g, 29%).

### II-2-2-4. Synthesis of 3,6-dibromo-4,5-difluorobenzene-1,2-diamine (**28**)

To a solution of compound **27** (6.3 g, 17.5 mmol) in ethanol (100 mL) and conc. HCl (60 mL) was added SnCl<sub>2</sub>•2H<sub>2</sub>O (39.5 g, 175 mmol) in several portions. The mixture was refluxed for 1 hr and stirred overnight at room temperature. Then, pH value of the mixture was adjusted to 8~9 by adding aqueous KOH solution. then the mixture was extracted with ethyl acetate three times. The combined organic phases were dried over anhydrous MgSO<sub>4</sub>. Further purification was run by silica column with petroleum hexane/CH<sub>2</sub>Cl<sub>2</sub> (1:1) to give a white-solid of

compound **28** (4.6 g, 88%).  $^1\text{H}$  NMR ( $\text{CDCl}_3$ , 300 MHz,  $\delta$ ): 3.85 (s, 4H).  $^{13}\text{C}$  NMR ( $\text{CDCl}_3$ , ppm): 142.99 (d,  $J = 18.11$  Hz), 141.06 (d,  $J = 17.65$  Hz), 129.78, 98.39 (t).  $^{19}\text{F}$  NMR ( $\text{CDCl}_3$ , ppm): -139.02. GC-MS ( $\text{M}^+$ ,  $\text{C}_6\text{H}_4\text{Br}_2\text{F}_2\text{N}_2$ ), calcd, 301.9; found: 302.

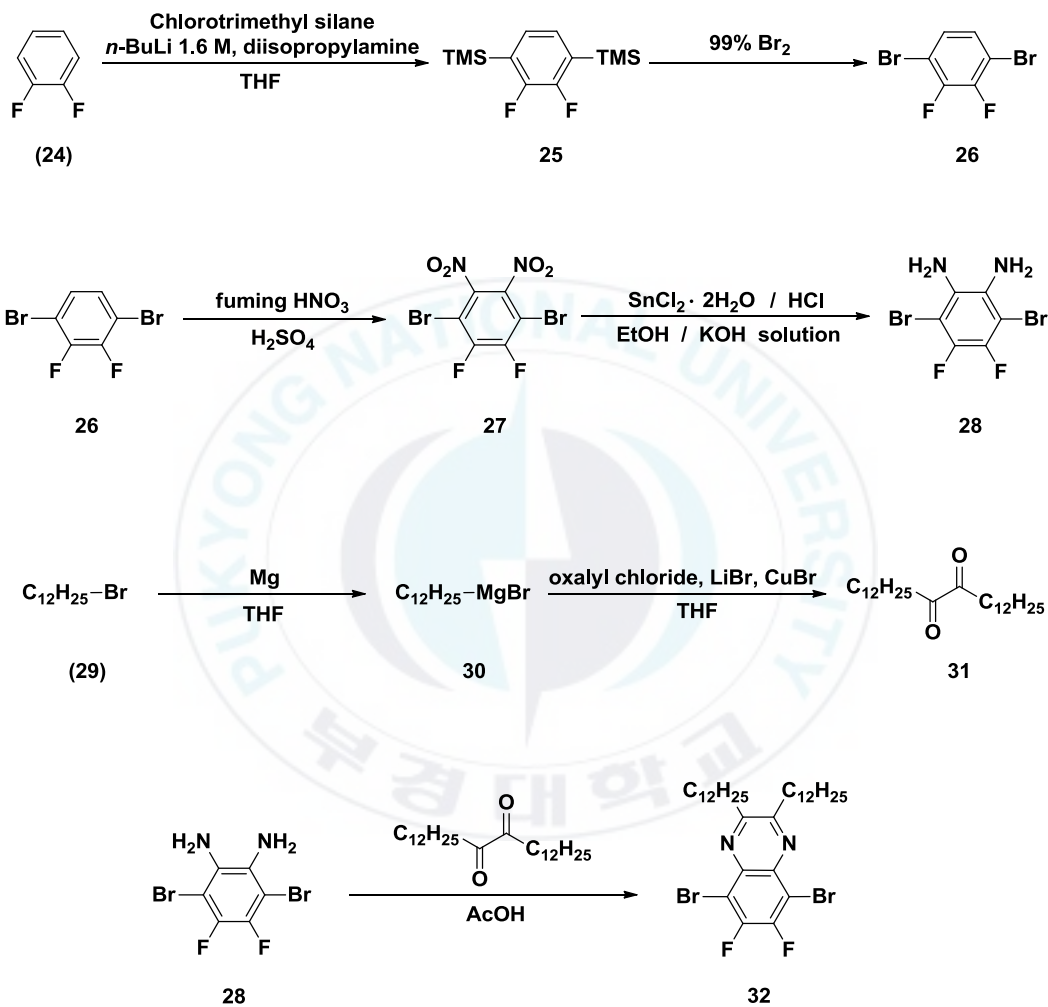
#### II-2-2-5. Synthesis of hexacosane-13,14-dione (**31**)

A Grignard reagent was prepared by the dropwise addition of the compound **29** (12.21 ml, 51 mmol) to a stirred suspension of iodine-activated magnesium (1.85 g, 76 mmol) in THF (30 mL). In a separate flask, LiBr (8.05 g, 93 mmol) in THF (150 mL) was added to a stirred suspension of CuBr (7.31 g, 51 mmol) in THF (150 mL) to form a pale green suspension. This mixture was then cooled to  $-78$  °C via a pentane/liquid nitrogen bath. The Grignard reagent was slowly added to the LiBr/CuBr suspension by cannula such that the temperature of the reaction mixture did not exceed  $-75$  °C. Oxalyl chloride (2 ml, 23 mmol) was then added slowly via syringe to maintain a temperature below  $-70$ °C. The mixture was stirred at  $-78$  °C for 60 min, allowed to warm to room temperature and quenched with saturated aqueous  $\text{NH}_4\text{Cl}$ . The organic layer was separated and the aqueous layer extracted repeatedly with ethyl acetate. The combined organic layers were dried with anhydrous  $\text{Na}_2\text{SO}_4$ , concentrated by rotary evaporation, and separated on a silica column using a 10:1 hexane/methylene chloride mixture. The compound **31** was obtained as a yellow solid (5.36 g, 58%).  $^1\text{H}$  NMR ( $\text{CDCl}_3$ ,

400 MHz,  $\delta$ ): 2.70 (t, 4H, J = 7.38 Hz), 1.54 (m, 4H, J = 7.12 Hz), 1.23 (m, 36H), 0.85 (t, 6H, J = 6.84 Hz)

#### II-2-2-6. Synthesis of 5,8-dibromo-6,7-difluoro-2,3-didodecylquinoxaline (32)

The compound **28** (2.2 g, 7.3 mmol) and compound **31** (3.48 g, 8.8 mmol) were dissolved in acetic acid (60 mL). The mixture was refluxed overnight. After cooling to room temperature, the resultant mixture was poured into water and extracted with ethylacetate. After dried over MgSO<sub>4</sub> and purified by silica column with petroleum hexane to give a white solid of compound **15** (3.67 g, 66%). <sup>1</sup>H NMR (CDCl<sub>3</sub>, 400MHz,  $\delta$ ): 3.03 (t, 4H, J = 7.66 Hz), 1.88 (m, 4H, J = 7.52 Hz), 1.24-1.44 (m, 36H), 0.86 (t, 6H, J = 6.84 Hz)



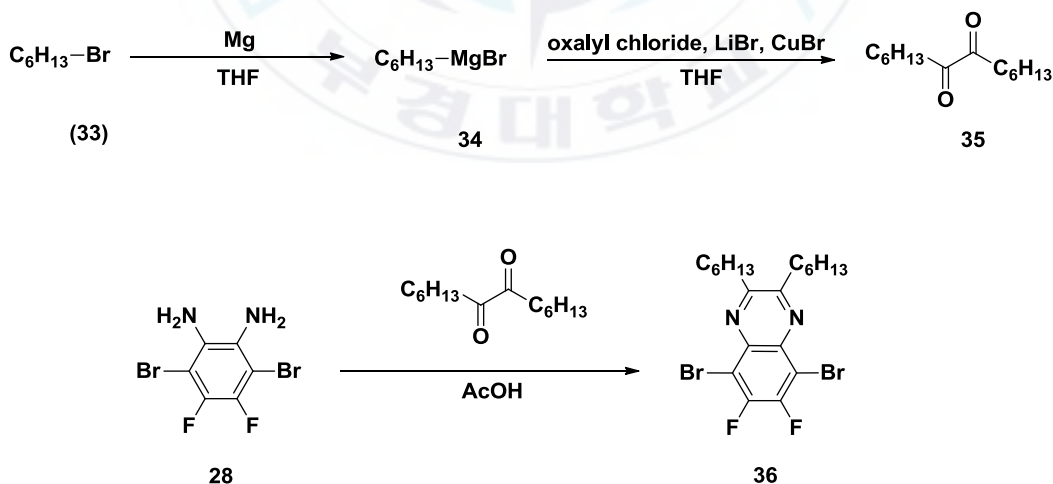
**Scheme 5.** Synthetic route of didodecyldifluoroquinoxaline (DFQx).

### II-2-2-7. Synthesis of tetradecane-7,8-dione (**35**)

A Grignard reagent was prepared by the dropwise addition of the respective hexyl bromide (152 mmol) to a stirred suspension of iodine-activated magnesium (4.0 g, 165 mmol) in THF (100 mL). In a separate flask, LiBr (25.5 g, 293 mmol) in THF (110 mL) was added to a stirred suspension of CuBr (21.1 g, 146 mmol) in THF (110 mL) to form a pale green suspension. This mixture was then cooled to -100 °C via a pentane/liquid nitrogen bath. The Grignard reagent was slowly added to the LiBr/CuBr suspension by cannula such that the temperature of the reaction mixture did not exceed -75 °C. Oxalyl chloride (7.77 g, 61.0 mmol) was then added slowly via syringe to maintain a temperature below -70 °C. The mixture was stirred at -90 to -95 °C for 60 min, allowed to warm to room temperature and quenched with saturated aqueous NH<sub>4</sub>Cl. The organic layer was separated and the aqueous layer extracted repeatedly with ethyl acetate. The combined organic layers were dried with anhydrous MgSO<sub>4</sub>, concentrated by rotary evaporation, and separated on a silica column using a petroleum ether/ethyl acetate (95:5) to give a yellow solid of compound **35** (10.91g, 76%). <sup>1</sup>H NMR (CDCl<sub>3</sub>, 400 MHz, δ): 0.86 (t, J = 7.2 Hz, 6H), 1.24 (m, 12H), 1.56 (p, J = 7.2 Hz, 4H), 2.72 (t, J = 7.2 Hz, 4H), <sup>13</sup>C NMR (CDCl<sub>3</sub>, ppm): δ 14.2, 22.7, 23.2, 29.0, 31.7, 36.3, 200.4.

### II-2-2-8. Synthesis of 5,8-dibromo-6,7-difluoro-2,3-dihexylquinoxaline (36).

The compound **28** (4.2 g, 14.0 mmol) and tetradecane-7,8-dione (3.81 g, 16.9 mmol) were dissolved in ethanol (15 mL) and acetic acid (15 mL). The mixture was refluxed overnight. After cooling to room temperature, the resultant mixture was poured into water and extracted with ethylacetate. After dried over  $\text{MgSO}_4$  and purified by silica column with petroleum hexane/ $\text{CH}_2\text{Cl}_2$  (10:1) to give a white solid of compound **36** (1.3 g, 18%).  $^1\text{H}$  NMR (600 MHz,  $\text{CDCl}_3$ ):  $\delta$  (ppm) = 7.92 (s, 2H), 7.66 (d, 4H), 7.40-7.42 (t, 2H), 7.35 (t, 4H),  $^{13}\text{C}$  NMR (125 MHz,  $\text{CDCl}_3$ ):  $\delta$  (ppm) = 154.1, 139.3, 138.0, 133.1, 130.3, 129.6, 128.4, 123.7. FT-IR (KBr,  $\text{v}/\text{cm}^{-1}$ ) = 3061, 1584, 1496, 1454, 1384, 1332, 1304, 1176, 1060, 1026, 988, 897, 828, 773, 656, 578, 536.



**Scheme 6.** Synthetic route of didohexyldifluoroquinoxaline (DFQx).

### II-2-2-9. Synthesis of 2,3-didodecyl-6,7-difluoro-5,8-di(thiophen-2-yl)quinoxaline (37)

To a solution of compound **32** (2.5 g, 3.8 mmol) and 2-tributylstannylthiophene (4.23 g, 11.4 mmol) in 60 mL *N,N'*-dimethylformamide (DMF) was added bis(triphenylphosphine)palladium(II) dichloride ( $\text{PdCl}_2(\text{PPh}_3)_2$ ) (81 mg, 0.11 mmol) under argon and heated at 85~90 °C for 24 h. Water was then added, and then the mixture was extracted with dichloromethane ( $\text{CH}_2\text{Cl}_2$ ). The organic phase was washed with water and dried over anhydrous  $\text{MgSO}_4$ . The solvent was removed by rotary evaporation and the residue was recrystallized from ethanol to give compound **37** as a yellow solid (2.04 g, 81%).  $^1\text{H}$  NMR ( $\text{CDCl}_3$ , 400 MHz,  $\delta$ ): 7.98 (d, 2H,  $J = 2.96$  Hz), 7.59 (d, 2H,  $J = 4.96$  Hz), 7.21 (t, 2H,  $J = 4.56$  Hz), 3.06 (t, 4H,  $J = 7.52$  Hz), 1.96 (m, 4H,  $J = 7.45$  Hz), 1.24-1.45 (m, 36H), 0.86 (t, 6H,  $J = 6.86$  Hz).  $^{13}\text{C}$  NMR ( $\text{CDCl}_3$ , 600MHz, ppm): 155.21, 149.62(d), 134.53, 131.01, 130.46, 130.41, 130.37, 129.52, 126.33, 117.51, 34.68, 31.92, 29.60(m), 28.14, 22.70, 14.14.

### II-2-2-10. Synthesis of 5,8-bis(5-bromothiophen-2-yl)-2,3-didodecyl-6,7-difluoroquinoxaline (38)

Compound **37** (2.0 g, 3.0 mmol) was dissolved in THF (60 mL) under nitrogen atmosphere, and NBS (1.1 g, 6.0 mmol) was added. The mixture was stirred at room temperature overnight. After that water (100 mL) was added to quench the

reaction, and then extracted with diethyl ether, washed with brine, and dried with anhydrous  $\text{MgSO}_4$ . The solvent was removed via rotary evaporation and subsequently purified by recrystallization to afford compound **38** as an orange solid (2.41 g, 95%).  $^1\text{H}$  NMR ( $\text{CDCl}_3$ , 400 MHz,  $\delta$ ): 7.75 (d, 2H,  $J = 4.00$  Hz), 7.14 (d, 2H,  $J = 4.04$  Hz), 3.08 (t, 4H,  $J = 7.66$  Hz), 1.97 (m, 4H,  $J = 7.46$  Hz), 1.23-1.46 (m, 36H), 0.85 (t, 6H,  $J = 6.84$  Hz).  $^{13}\text{C}$  NMR ( $\text{CDCl}_3$ , 600 MHz, ppm): 155.42, 149.46(d), 133.58, 132.60, 130.35, 129.03, 118.56, 116.61, 34.75, 31.93, 29.63(m), 28.14, 22.70, 14.14.

#### **II-2-2-11. Synthesis of 5-(5-bromothiophen-2-yl)-2,3-didodecyl-6,7-difluoro-8-(thiophen-2-yl)quinoxaline (39)**

Compound **37** (2.5 g, 3.75 mmol) was dissolved in THF (60 mL) under nitrogen atmosphere, and NBS (0.67 g, 3.75 mmol) was added. The mixture was stirred at room temperature overnight. After that water (100 mL) was added to quench the reaction, and then extracted with diethyl ether, washed with brine, and dried with anhydrous  $\text{MgSO}_4$ . The solvent was removed via rotary evaporation and subsequently purified by recrystallization to afford compound **39** as an orange solid (1.5 g, 58%).  $^1\text{H}$  NMR ( $\text{CDCl}_3$ , 400MHz,  $\delta$ ): 7.75 (d, 2H,  $J = 4.00$  Hz), 7.14 (d, 2H,  $J = 4.04$  Hz), 3.08 (t, 4H,  $J = 7.66$  Hz), 1.97 (m, 4H,  $J = 7.46$  Hz), 1.23-1.46 (m, 36H), 0.85 (t, 6H,  $J = 6.84$  Hz).  $^{13}\text{C}$  NMR ( $\text{CDCl}_3$ , 600MHz, ppm): 155.42, 149.46(d), 133.58, 132.60, 130.35, 129.03, 118.56, 116.61, 34.75, 31.93,

29.63(m), 28.14, 22.70, 14.14.

**II-2-2-12. Synthesis of 6,7-difluoro-2,3-dihexyl-5,8-di(thiophen-2-yl)quinoxaline (40)**

Compound **36** (5.63 g, 11.44 mmol), 2-(tributylstanny)thiophene (17.08 g, 6.42 mmol), and Pd(PPh<sub>2</sub>)Cl<sub>2</sub> were charged in a 250 mL round-bottomed flask, followed by addition of 75 mL of THF. The mixture was heated to 110 °C and maintained for 24 h. After cooling, the product was obtained yellow crystal by column chromatography (silica gel, dichloromethane/ hexane ) 1 : 20) yielded compound **40** (5.43g, 10.71 mmol, 93.6%) <sup>1</sup>H NMR (400MHz, CDCl<sub>3</sub>) δ 7.10 (m, 9H), δ 7.24 (m, 6H), δ 7.46 (m, 2H); <sup>13</sup>C NMR (400 MHz, CDCl<sub>3</sub>) δ 122.33, 123.13, 123.88, 124.10, 124.53, 124.53, 126.83, 128.08, 128.64, 129.41, 144.34, 147.28, 147.5

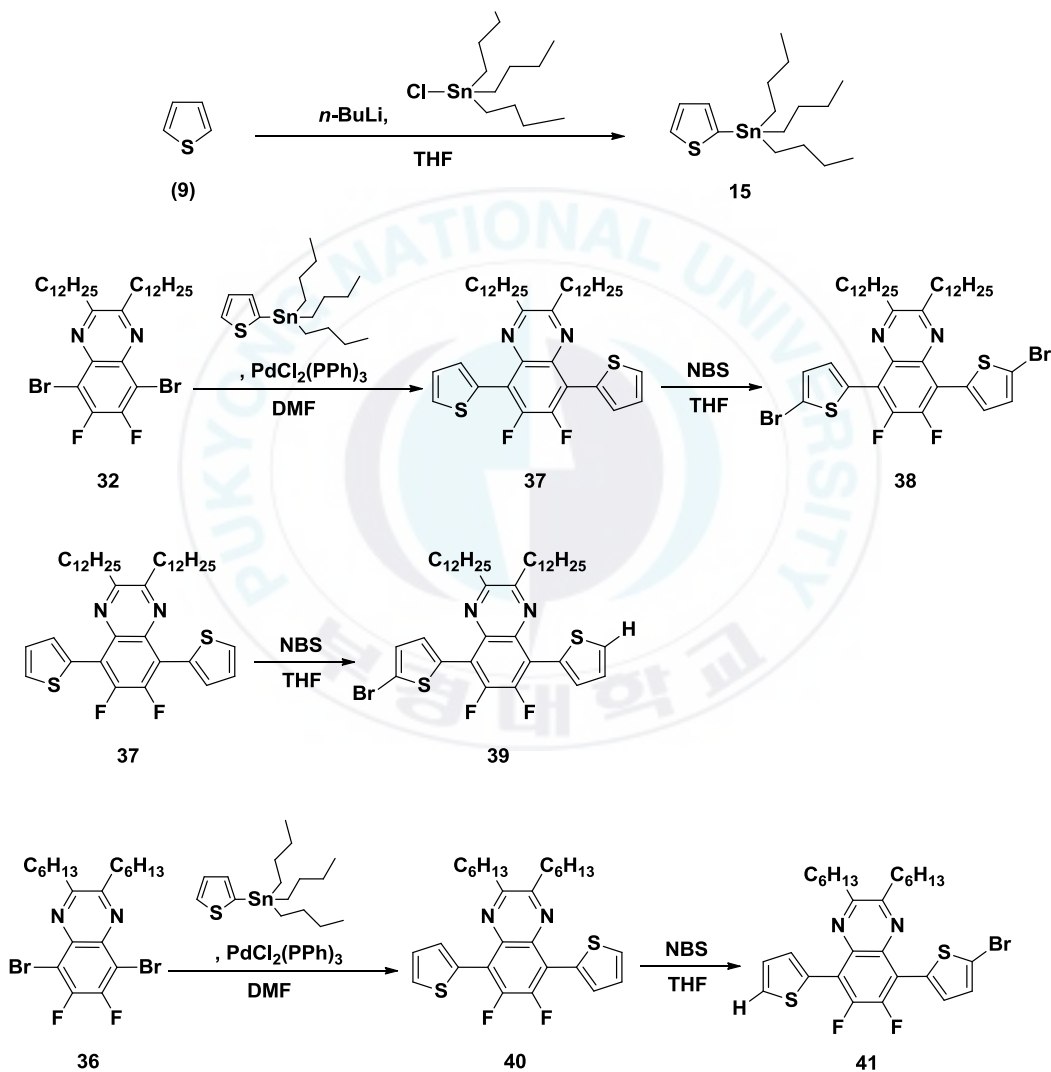
**II-2-2-13. Synthesis of 5-(5-bromothiophen-2-yl)-2,3-dihexyl-6,7-difluoro-8-(thiophen-2-yl)quinoxaline (41)**

NBS (1.00 g, 5.59 mmol) was added and stirred solution of compound **40** (2.78 g, 5.59 mmol) in THF (80 mL). The mixture was stirred at room temperature overnight and then extracted with diethyl ether. After being washed with water and brine, the organic phase were evaporated under reduced pressure and column chromatography yielded compound **41** (1.80 g, 3.12 mmol, 55.92%) of a yellow

solid.  $^1\text{H}$  NMR ( $\text{CDCl}_3$ , 400MHz,  $\delta$ ): 7.18 (d, 2H), 6.73 (d, 2H), 3.86 (s, 2H).

$^{13}\text{C}$  NMR ( $\text{CDCl}_3$ , 600MHz,  $\delta$ ): 138.79 (q), 128.46 (t), 125.70 (t), 109.80 (q),

29.47 (s).

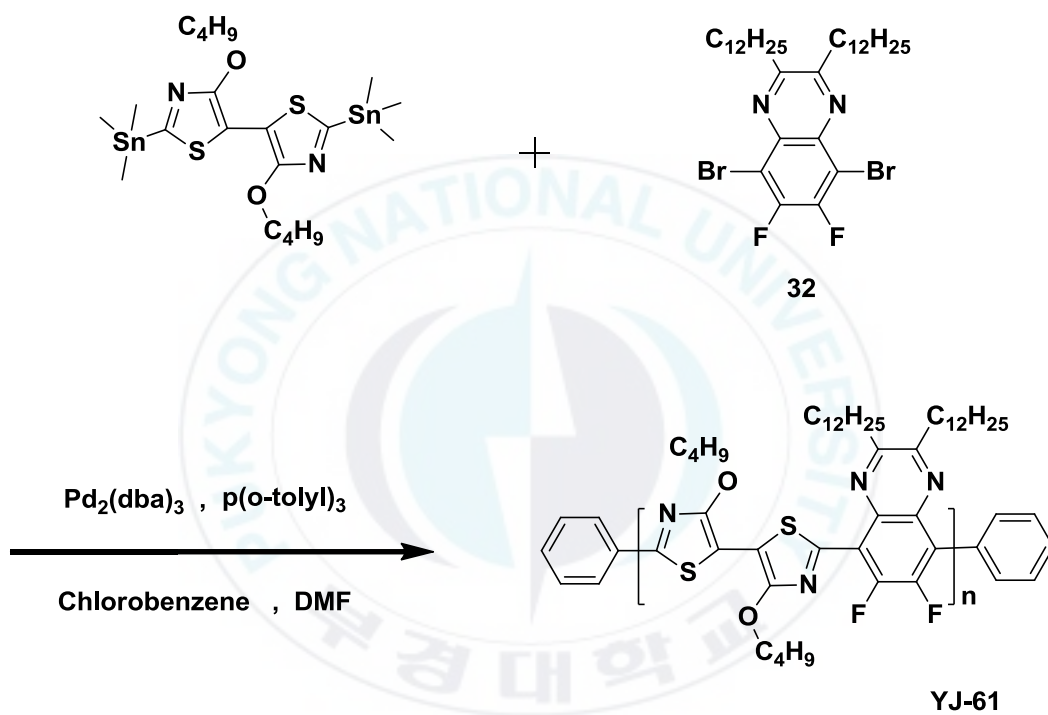


**Scheme 7.** Synthetic route of mono-Br or di-Br dithienoquinoxaline (DTDFQx).

## II-3. Synthesis of polymer

### II-3-1. Synthesis of poly[4,4'-dibutoxy-2-(2,3-didodecyl-6,7-difluoro-8-phenylquinoxaline-5-yl)-2'-phenyl-5,5'-bithiazole] (YJ-61)

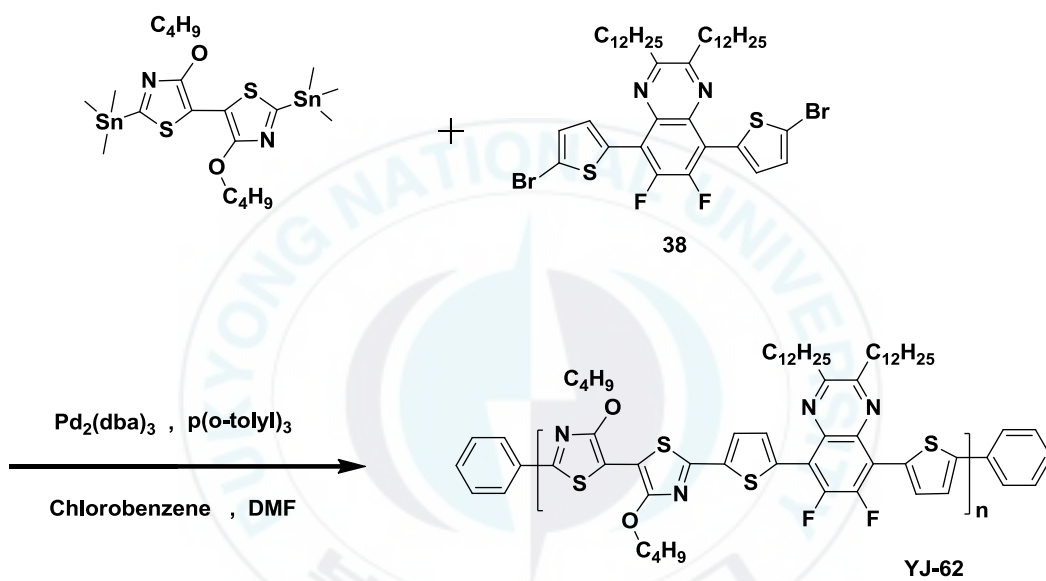
In a 25 mL dry flask, (4,4'-dibutoxy-2,2'-bis(trimethylstannyl)-5,5'-bithiazole (0.4557 g, 0.7 mmol) and 5,8-dibromo-2,3-didodecyl-6,7-difluoroquinoxaline (**32**) (0.4623 g, 0.7 mmol) were dissolved in a mixture of degassed chlorobenzene (8 mL) and *N,N*-dimethylformamide (2 mL) under argon atmosphere. *P(o-tolyl)*<sub>3</sub> (85 mg, 0.28 mmol) and tris(dibenzylideneacetone) dipalladium (0) (Pd<sub>2</sub>(dba)<sub>3</sub>) (32 mg, 0.035 mmol) were added. And then, the mixture compounds were strongly stirred at 100~110 °C for 48~72 hr. After cooling down, the solution was poured into methanol. The polymer was collected by filtration and was Soxhlet-extracted in order with methanol, hexane, and then with chloroform. The chloroform solution was concentrated to a small volume, and the polymer was precipitated by pouring this solution into methanol. Finally, the polymer was collected by filtration, dried under vacuum at 50 °C overnight and afforded PbiTz-DFQ<sub>x</sub> (488 mg) in yield 85.72%.



**Scheme 8.** Synthetic route of PbiTz-DFQx (YJ-61).

### II-3-2. Synthesis of poly[4,4'-dibutoxy-2-(5-(2,3-didodecyl-6,7-difluoro-8-(5-phenylthiophen-2-yl)quinoxaline-5-yl)-2'-phenyl-5,5'-bithiazole)(YJ-62)

In a 25 mL dry flask, (4,4'-dibutoxy-2,2'-bis(trimethylstannyl)-5,5'-bithiazole (0.4557 g, 0.7 mmol) and 5,8-bis(5-bromothiophen-2-yl)-2,3-didodecyl-6,7-difluoroquinoxaline (**38**) (0.5773 g, 0.7 mmol) were dissolved in a mixture of degassed chlorobenzene (8 mL) and *N,N'*-dimethylformamide (2 mL) under argon atmosphere.  $P(o\text{-tolyl})_3$  (85 mg, 0.28 mmol) and tris(dibenzylideneacetone)dipalladium (0) ( $\text{Pd}_2(\text{dba})_3$ ) (32 mg, 0.035 mmol) were added. And then, the mixture compounds were strongly stirred at 100~110 °C for 48~72 hr. After cooling down, the solution was poured into methanol. The polymer was collected by filtration and was Soxhlet-extracted in order with methanol, hexane, and then with chloroform. The chloroform solution was concentrated to a small volume, and the polymer was precipitated by pouring this solution into methanol. Finally, the polymer was collected by filtration, dried under vacuum at 50 °C overnight and afforded PbiTz-DTDFQx (621 mg) in yield 90.50%.

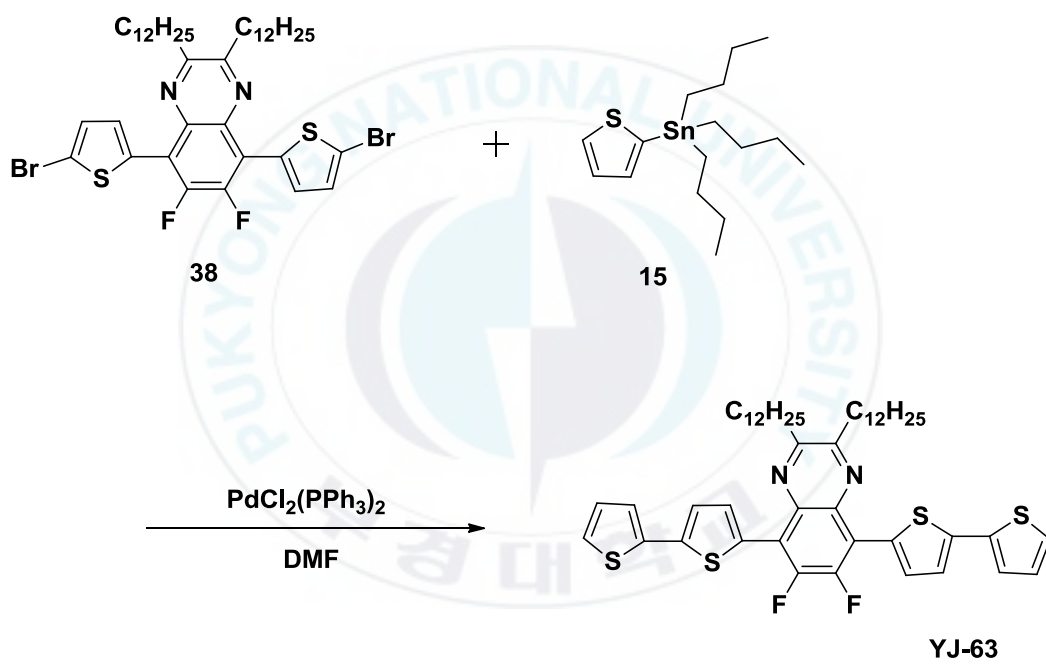


**Scheme 9.** Synthetic route of PbiTz-DTDFQx (**YJ-62**).

## II-4. Synthesis of small molecular

### II-4-1. Synthesis of 5,8-di([2,2'-bithiophene]-5-yl)-2,3-didodecyl-6,7-difluoroquinoxaline (YJ-63)

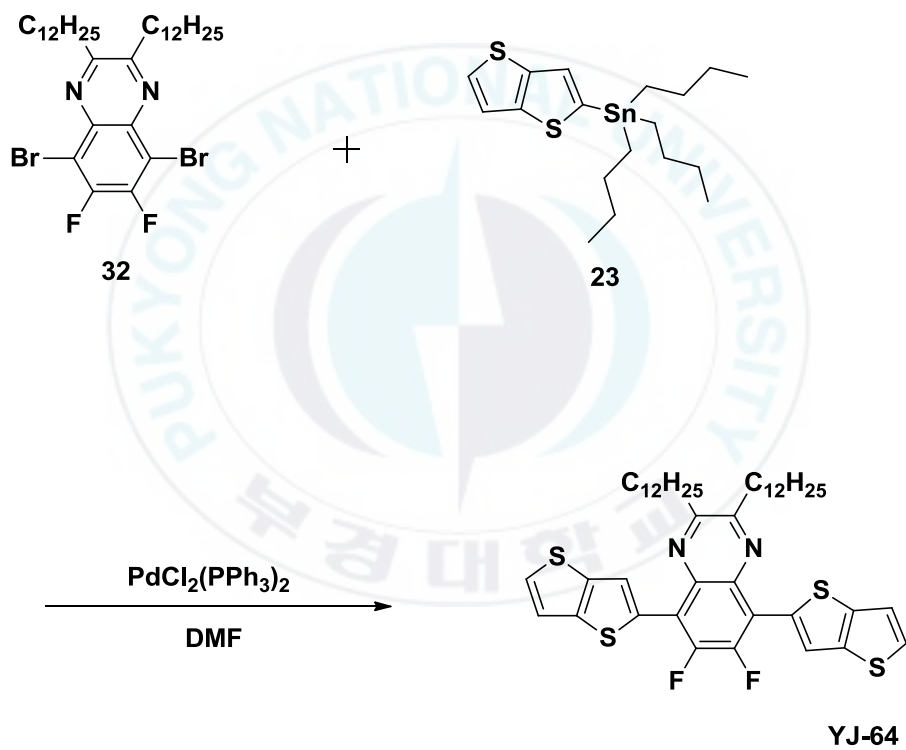
In a 100 mL dry flask, 5,8-bis(5-bromothiophen-2-yl)-2,3-didodecyl-6,7-difluoroquinoxaline (**38**) (2.11 g, 2.56 mmol), tributyl(thiophen-2-yl)stannane (**15**) (2.87 g, 7.69 mmol) and bis(triphenylphosphine)palladium(II) dichloride (53.5 mg, 0.072 mmol) were dissolved in *N,N'*-dimethylformamide (15 mL) under argon atmosphere. And then, the mixture was stirred at 85~90 °C overnight. After that water (100 mL) was added to quench the reaction, and then extracted with methylene chloride, washed with brine, and dried with anhydrous MgSO<sub>4</sub>. The solvent was removed through rotary evaporation and subsequently purified by silica column with petroleum hexane/CH<sub>2</sub>Cl<sub>2</sub> (1:1) to give an orange solid of **YJ-63** (1.81 g, 85%).



**Scheme 10.** Synthetic route of 2TQx (**YJ-63**).

#### II-4-2. Synthesis of 2,3-didodecyl-6,7-difluoro-5,8-bis(thieno[3,2-*b*]thiophen-2-yl)quinoxaline (YJ-64)

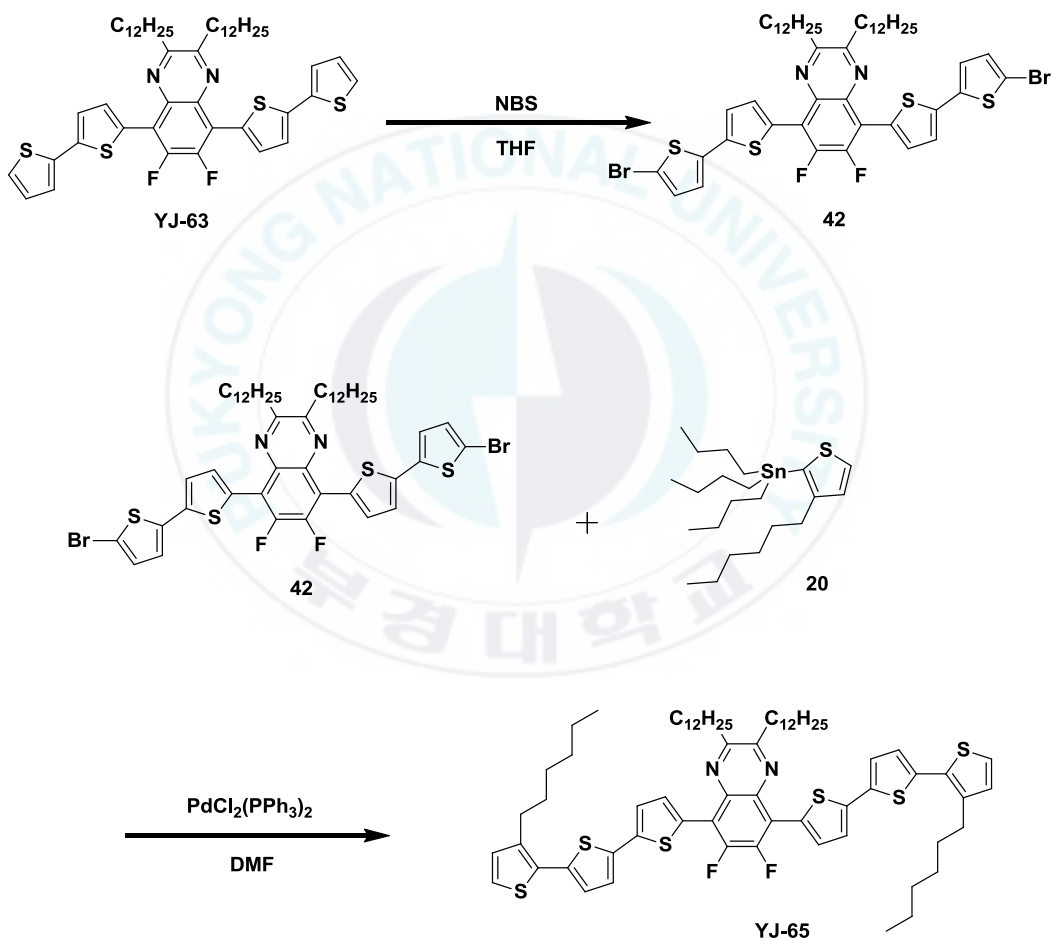
In a 100 mL dry flask, 5,8-dibromo-2,3-didodecyl-6,7-difluoroquinoxaline (**32**) (2.16 g, 3.29 mmol), tributyl(thieno[3,2-*b*]thiophen-2-yl)stannane (**23**) (4.24 g, 9.86 mmol) and bis(triphenylphosphine)palladium(II) dichloride (69.0 mg, 0.099 mmol) were dissolved in *N,N*-dimethylformamide (15 mL) under argon atmosphere. And then, the mixture was stirred at 85~90 °C overnight. After that water (100 mL) was added to quench the reaction, and then extracted with methylene chloride, washed with brine, and dried with anhydrous MgSO<sub>4</sub>. The solvent was removed through rotary evaporation and subsequently purified by silica column with petroleum hexane/CH<sub>2</sub>Cl<sub>2</sub> (5:1) to give an orange solid of **YJ-64** (1.96 g, 78%).



**Scheme 11.** Synthetic route of TTQx (YJ-64).

### II-4-3. Synthesis of 2,3-didodecyl-6,7-difluoro-5,8-bis(3''-hexyl-[2,2':5',2''-terthiophen]-5-yl)quinoxaline (YJ-65)

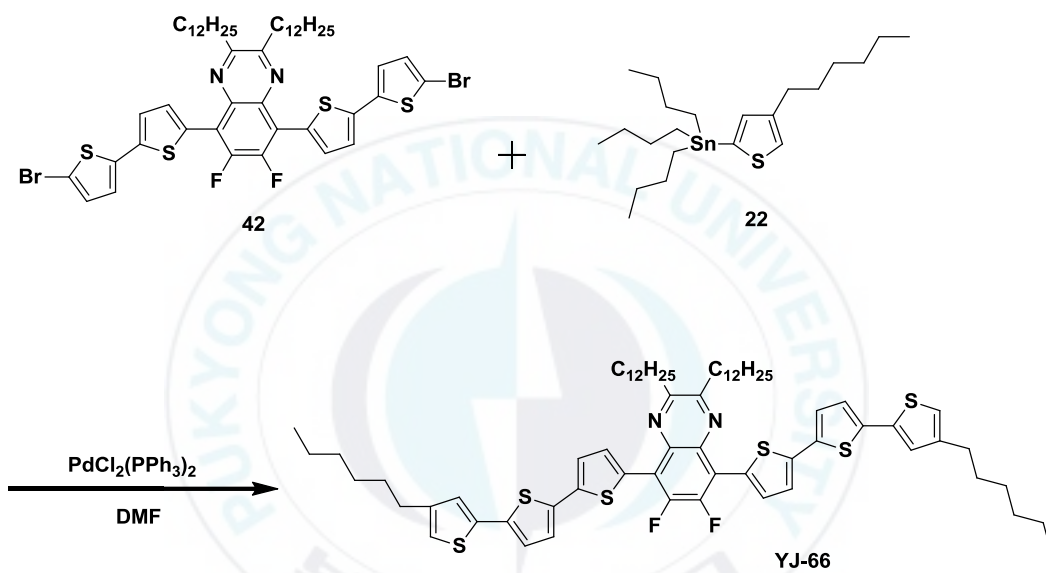
In a 100 mL dry flask, YJ-63 (1.00 g, 1.20 mmol) and N-bromosuccinimide (0.43 g, 2.40 mmol) were dissolved in THF (20 mL) under argon atmosphere. And then, the mixture was stirred at room temperature overnight. Water was then added, and then the mixture was extracted with dichloromethane (CH<sub>2</sub>Cl<sub>2</sub>). The organic phase was washed with water and dried over anhydrous MgSO<sub>4</sub>. The solvent was removed by rotary evaporation and the residue was purified by silica column with petroleum hexane/CHCl<sub>3</sub> (7:1) to give an orange solid of (**42**) (1.16g, 98.90%). After that, In a 100 mL dry flask, 5,8-bis(5'-bromo-[2,2'-bithiophen]-5-yl)-2,3-didodecyl-6,7-difluoroquinoxaline (**42**) (0.90 g, 0.91 mmol), tributyl(3-hexylthiophen-2yl)stannane (**20**) (1.24 g, 2.72 mmol) and bis(triphenylphosphine) palladium(II) dichloride (19.4 mg, 0.072 mmol) were dissolved in *N,N'*-dimethylformamide (15 mL) under argon atmosphere. And then, the mixture was stirred at 85~90 °C overnight. And then, the mixture was extracted with dichloromethane (CH<sub>2</sub>Cl<sub>2</sub>). The organic phase was washed with water and dried over anhydrous MgSO<sub>4</sub>. The solvent was removed by rotary evaporation and the residue was purified by silica column with petroleum hexane/CHCl<sub>3</sub> (7:1) to give a red solid of YJ-65 (0.61 g, 57.66%).



**Scheme 12.** Synthetic route of 3TDFQx (In) (YJ-65).

#### II-4-4. Synthesis of 2,3-didodecyl-6,7-difluoro-5,8-bis(4''hexyl-[2,2':5',2''-terthiophen]-5-yl)quinoxaline (YJ-66)

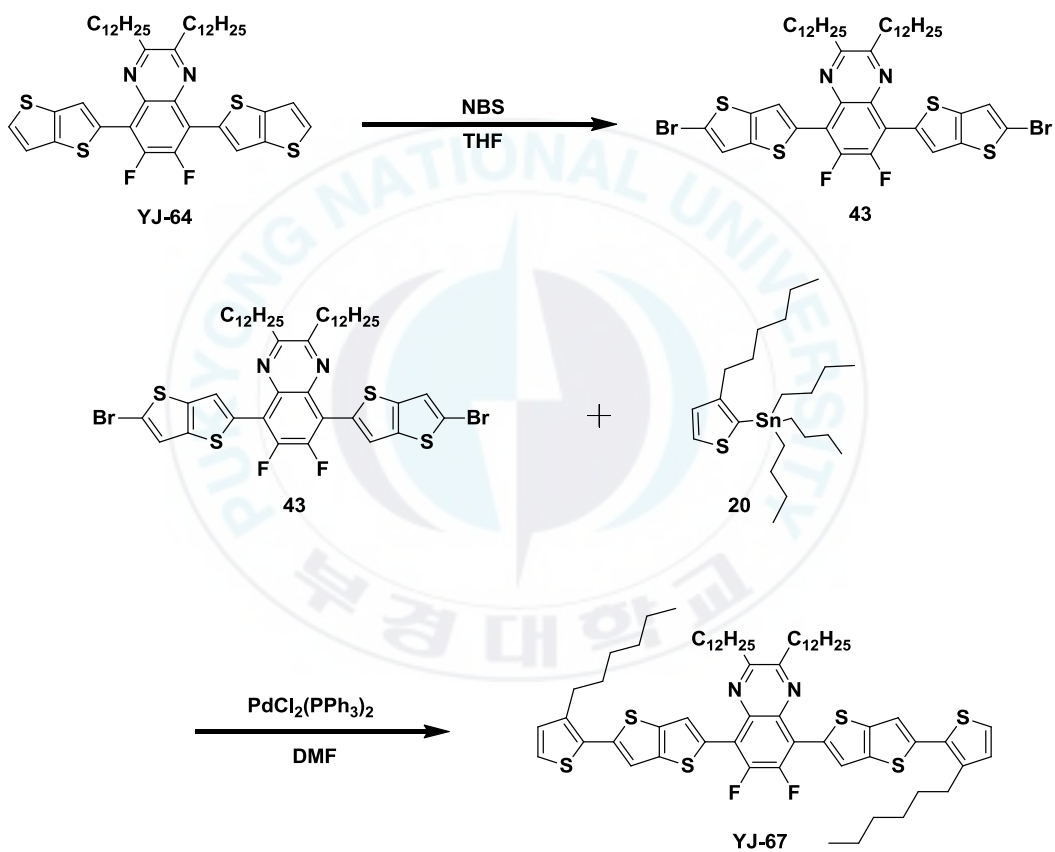
In a 100 mL dry flask, 5,8-bis(5'-bromo-[2,2'-bithiophen]-5-yl)-2,3-didodecyl-6,7-difluoroquinoxaline (**42**) (0.90 g, 0.91 mmol), tributyl(3-hexylthiophen-2-yl)stannane (**22**) (1.24 g, 2.72 mmol) and bis(triphenylphosphine) palladium(II) dichloride (19.4 mg, 0.072 mmol) were dissolved in *N,N'*-dimethylformamide (15 mL) under argon atmosphere. And then, the mixture was stirred at 85~90 °C overnight. And then, the mixture was extracted with chloroform (CHCl<sub>3</sub>). The organic phase was washed with water and dried over anhydrous MgSO<sub>4</sub>. The solvent was removed by rotary evaporation and the residue was purified by silica column with petroleum hexane/CHCl<sub>3</sub> (7:1) to give a red solid of **YJ-65** (0.67 g, 63.36%).



**Scheme 13.** Synthetic route of 3TDFQx (Out) (**YJ-66**).

#### II-4-5. Synthesis of 2,3-didodecyl-6,7-difluoro-5,8-bis(5-(3-hexylthiophen-2-yl)thieno[3,2-b]thiophen-2-yl)quinoxaline (YJ-67)

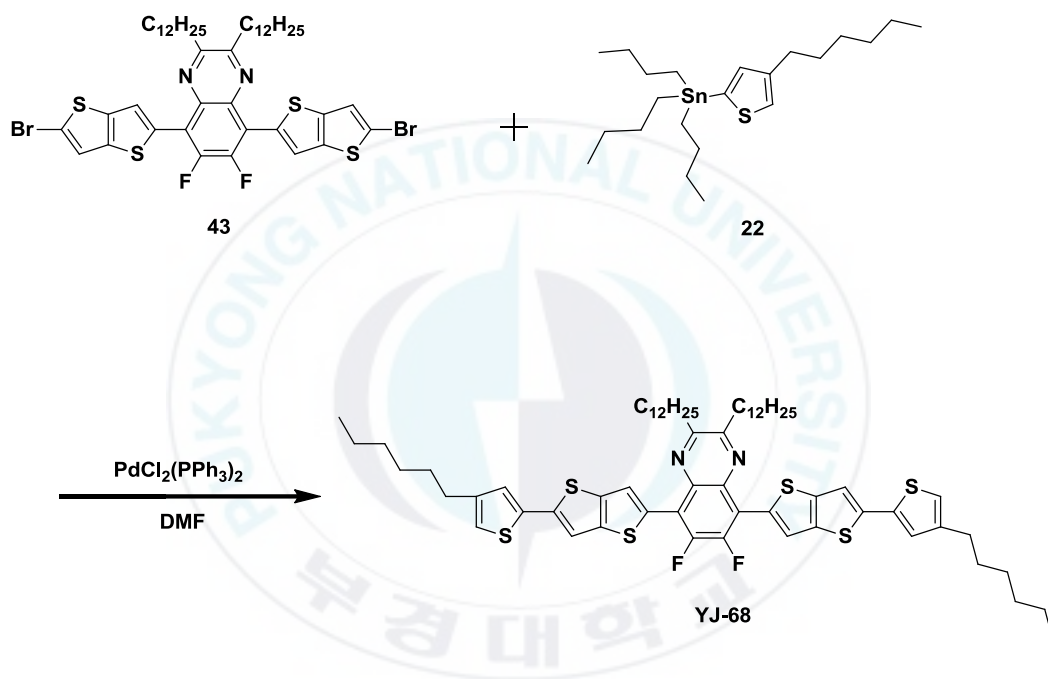
In a 100 mL dry flask, **YJ-64** (1.89 g, 2.42 mmol) and N-bromosuccinimide (0.86 g, 4.80 mmol) were dissolved in THF (30 mL) under argon atmosphere. And then, the mixture was stirred at room temperature overnight. Water was then added, and then the mixture was extracted with dichloromethane (CH<sub>2</sub>Cl<sub>2</sub>). The organic phase was washed with water and dried over anhydrous MgSO<sub>4</sub>. The solvent was removed by rotary evaporation and the residue was purified by silica column with petroleum hexane/CH<sub>2</sub>Cl<sub>2</sub> (7:1) to give an orange solid of (**43**) (1.60 g, 70.00%). After that, In a 100 mL dry flask, 5,8-bis(5-bromothieno[3,2-b]thiophen-2-yl)-2,3-didodecyl-6,7-difluoroquinoxaline (**43**) (0.60 g, 0.64 mmol), tributyl(3-hexylthiophen-2-yl)stannane (**20**) (0.87 g, 1.92 mmol) and bis(triphenylphosphine) palladium(II) dichloride (13.7 mg, 0.019 mmol) were dissolved in *N,N'*-dimethylformamide (15 mL) under argon atmosphere. And then, the mixture was stirred at 85~90 °C overnight. And then, the mixture was extracted with chloroform (CHCl<sub>3</sub>). The organic phase was washed with water and dried over anhydrous MgSO<sub>4</sub>. The solvent was removed by rotary evaporation and the residue was purified by silica column with petroleum hexane/CHCl<sub>3</sub> (7:1) to give a red solid of **YJ-67** (0.42 g, 59.02%).



**Scheme 14.** Synthetic route of T-TT-DFQx (In) (YJ-67).

#### II-4-6. Synthesis of 2,3-didodecyl-6,7-difluoro-5,8-bis(5-(4-hexylthiophen-2-yl)thieno[3,2-b]thiophen-2-yl)quinoxaline (YJ-68)

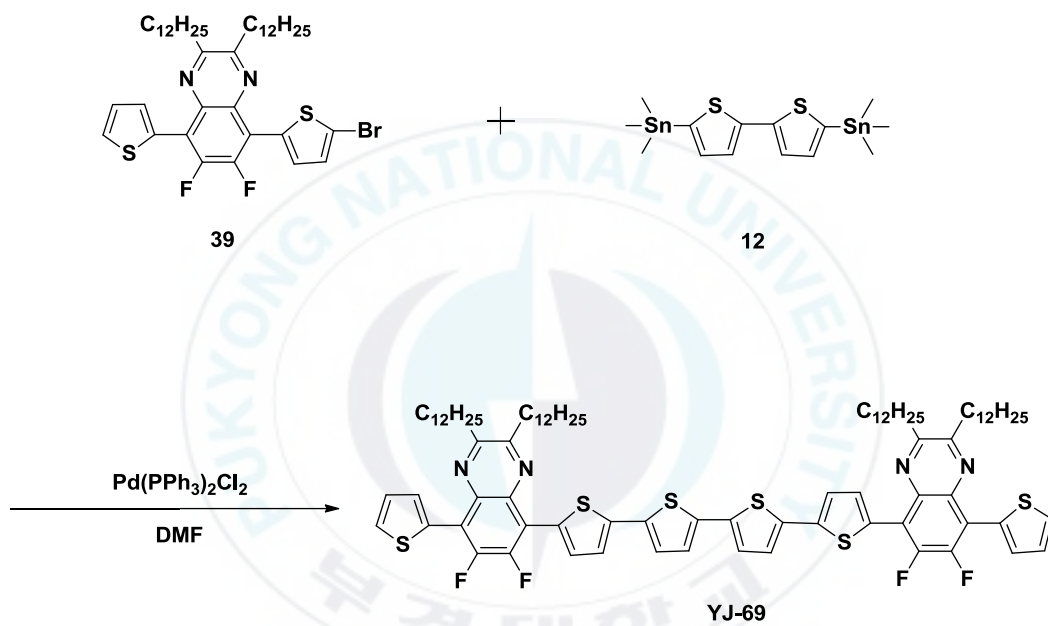
In a 100 mL dry flask, 5,8-bis(5-bromothieno[3,2-b]thiophen]-2-yl)-2,3-didodecyl-6,7-difluoroquinoxaline (**43**) (0.60 g, 0.64 mmol), tributyl(4-hexylthiophen-2-yl)stannane (**22**) (0.87 g, 1.92 mmol) and bis(triphenylphosphine) palladium(II) dichloride (13.7 mg, 0.019 mmol) were dissolved in *N,N*-dimethylformamide (15 mL) under argon atmosphere. And then, the mixture was stirred at 85~90 °C overnight. And then, the mixture was extracted with chloroform (CHCl<sub>3</sub>). The organic phase was washed with water and dried over anhydrous MgSO<sub>4</sub>. The solvent was removed by rotary evaporation and the residue was purified by silica column with petroleum hexane/CHCl<sub>3</sub> (7:1) to give a red solid of **YJ-68** (0.48 g, 67.00%).



**Scheme 15.** Synthetic route of T-TT-DFQx (Out) (**YJ-68**).

#### II-4-7. Synthesis of 5,5''-bis(2,3-didodecyl-6,7-difluoro-8-(thiophen-2-yl)quinoxalin-5-yl)-2,2':5',2'':5'',2'''-quaterthiophene (YJ-69)

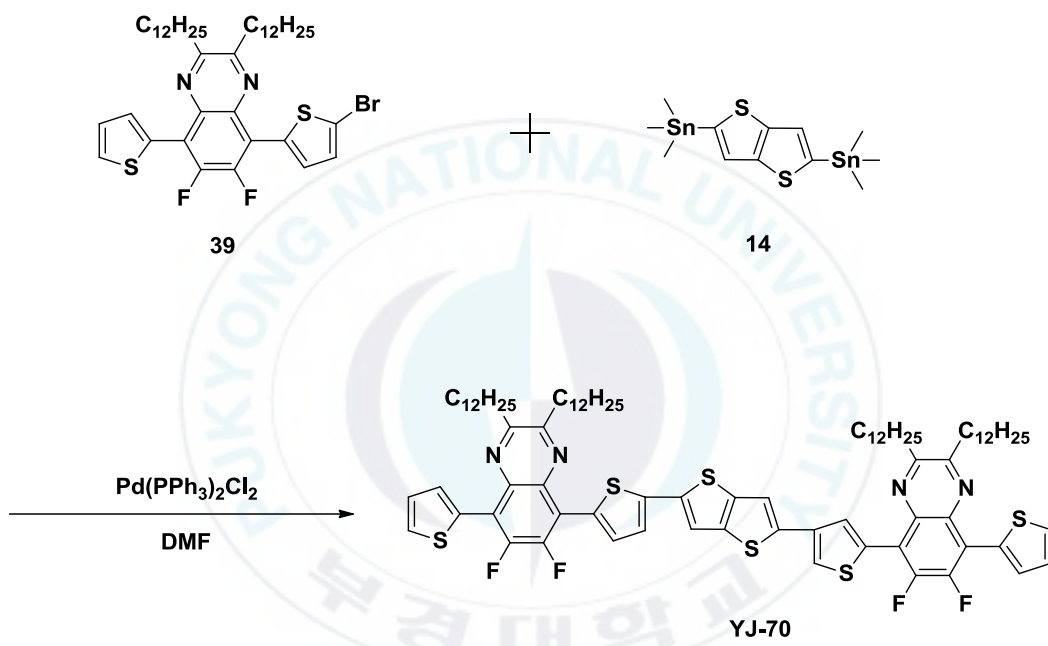
In a 100 mL dry flask, 5-(5-bromothiophen-2-yl)-2,3-didodecyl-6,7-difluoro-8-(thiophen-2-yl)quinoxaline (**39**) (0.69 g, 0.935 mmol), 5,5'-bis(trimethylstannyl)-2,2'-bithiophene (**12**) (0.2 g, 0.406 mmol) and bis(triphenylphosphine)palladium(II) dichloride (6.5 mg, 0.00935 mmol) were dissolved in *N,N*-dimethylformamide (10 mL) under argon atmosphere. And then, the mixture was stirred at 85~90 °C overnight. And then, the mixture was extracted with chloroform (CHCl<sub>3</sub>). The organic phase was washed with water and dried over anhydrous MgSO<sub>4</sub>. The solvent was removed by rotary evaporation and the residue was purified by silica column with petroleum hexane/CHCl<sub>3</sub> (6:1) to give a red solid of **YJ-69** (0.40 g, 65.76%).



**Scheme 16.** Synthetic route of biT(DTDFQ<sub>x</sub>)<sub>2</sub> (**YJ-69**).

**II-4-8. Synthesis of 5-(4-(5-(5-(2,3-didodecyl-6,7-difluoro-8-(thiophen-2-yl)quinoxalin-5-yl)thiophen-2-yl)thieno[3,2-*b*]thiophen-2-yl)thiophen-2-yl)2,3-didodecyl-6,7-difluoro-8-(thiophen-2-yl)quinoxaline (YJ-70)**

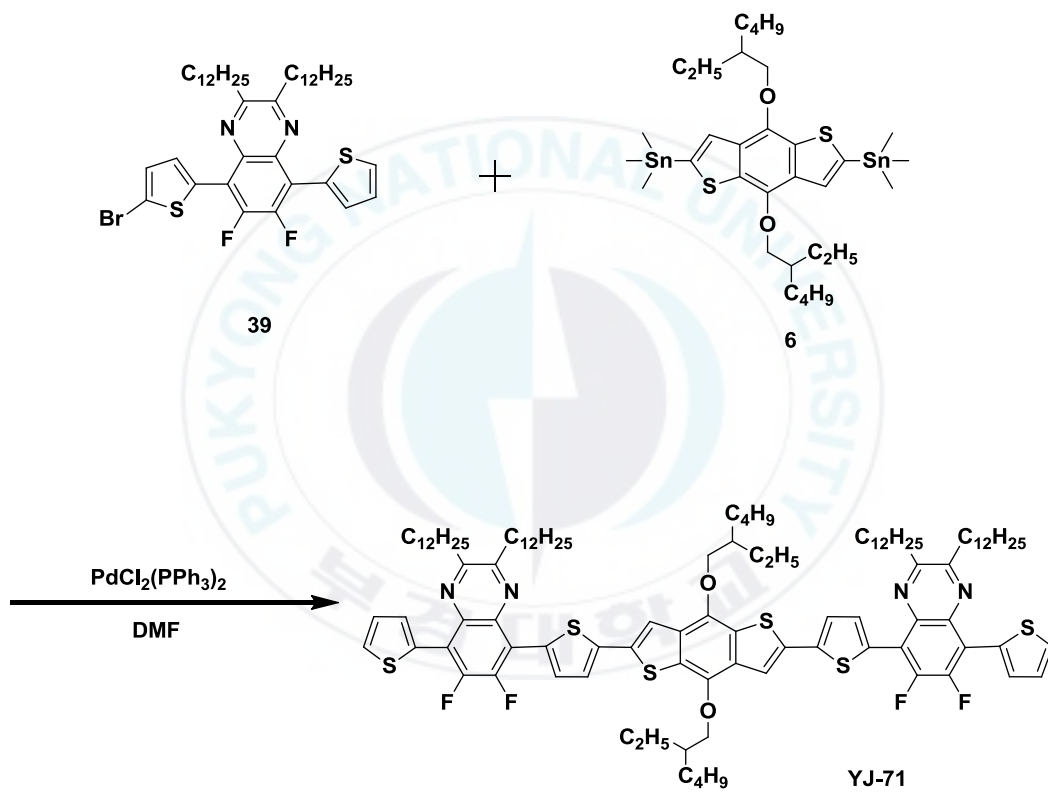
In a 100 mL dry flask, 5-(5-bromothiophen-2-yl)-2,3-didodecyl-6,7-difluoro-8-(thiophen-2-yl)quinoxaline (**39**) (0.76 g, 1.03 mmol), 2,5-bis(trimethylstannyl)thieno[3,2-*b*]thiophene (**14**) (0.2 g, 0.42 mmol) and bis(triphenylphosphine) palladium(II) dichloride (7.3 mg, 0.0103 mmol) were dissolved in *N,N'*-dimethylformamide (10 mL) under argon atmosphere. And then, the mixture was stirred at 85~90 °C overnight. And then, the mixture was extracted with chloroform (CHCl<sub>3</sub>). The organic phase was washed with water and dried over anhydrous MgSO<sub>4</sub>. The solvent was removed by rotary evaporation and the residue was purified by silica column with petroleum hexane/CHCl<sub>3</sub> (4:1) to give a red solid of **YJ-70** (0.23 g, 37.24%).



**Scheme 17.** Synthetic route of TT(DTDFQ<sub>x</sub>)<sub>2</sub> (**YJ-70**).

**II-4-9. Synthesis of 8,8'-(5,5'-(4,8-bis((2-ethylhexyl)oxy)benzo[1,2-*b*:4,5-*b'*']dithiophene-2,6-diyl)bis(thiophene-5,2-diyl))bis(2,3-didodecyl-6,7-difluoro-5-(thiophen-2-yl)quinoxaline (YJ-71)**

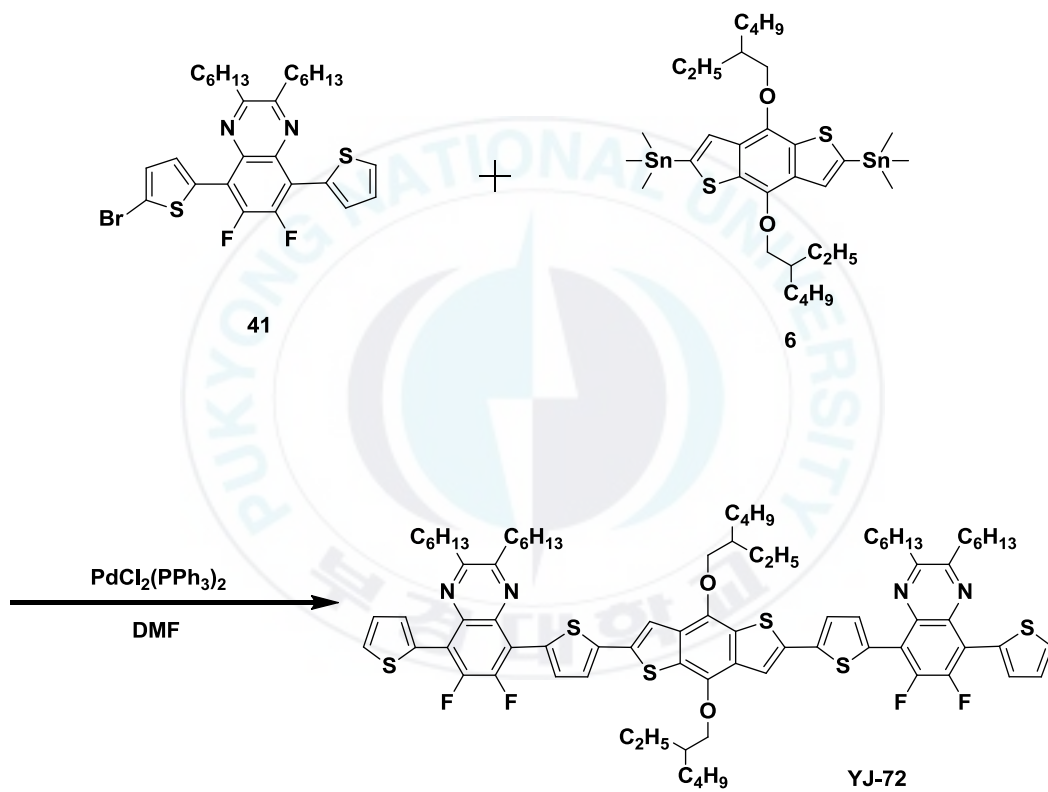
In a 100 mL dry flask, 5-(5-bromothiophen-2-yl)-2,3-didodecyl-6,7-difluoro-8-(thiophen-2-yl)quinoxaline (**39**) (0.67 g, 0.89 mmol), (4,8-bis((2-ethylhexyl)oxy)benzo[1,2-*b*:4,5-*b'*']dithiophene-2,6-diyl)bis(trimethylstannane) (**6**) (0.3 g, 0.38 mmol) and bis(triphenylphosphine) palladium(II) dichloride (6.2 mg, 0.0089 mmol) were dissolved in *N,N'*-dimethylformamide (10 mL) under argon atmosphere. And then, the mixture was stirred at 85~90 °C overnight. And then, the mixture was extracted with chloroform (CHCl<sub>3</sub>). The organic phase was washed with water and dried over anhydrous MgSO<sub>4</sub>. The solvent was removed by rotary evaporation and the residue was purified by silica column with petroleum hexane/CH<sub>2</sub>Cl<sub>2</sub> (6:1) to give a red solid of **YJ-71** (0.41 g, 60.72%).



**Scheme 18.** Synthetic route of EH-BDT(DTDFDDoQx)<sub>2</sub> (YJ-71).

**II-4-10. Synthesis of 8,8'-(5,5'-(4,8-bis((2-ethylhexyl)oxy)benzo[1,2-*b*:4,5-*b'*])dithiophene-2,6-diyl)bis(thiophene-5,2-diyl))bis(2,3-dihexcyl-6,7-difluoro-5-(thiophen-2-yl)quinoxaline (YJ-72)**

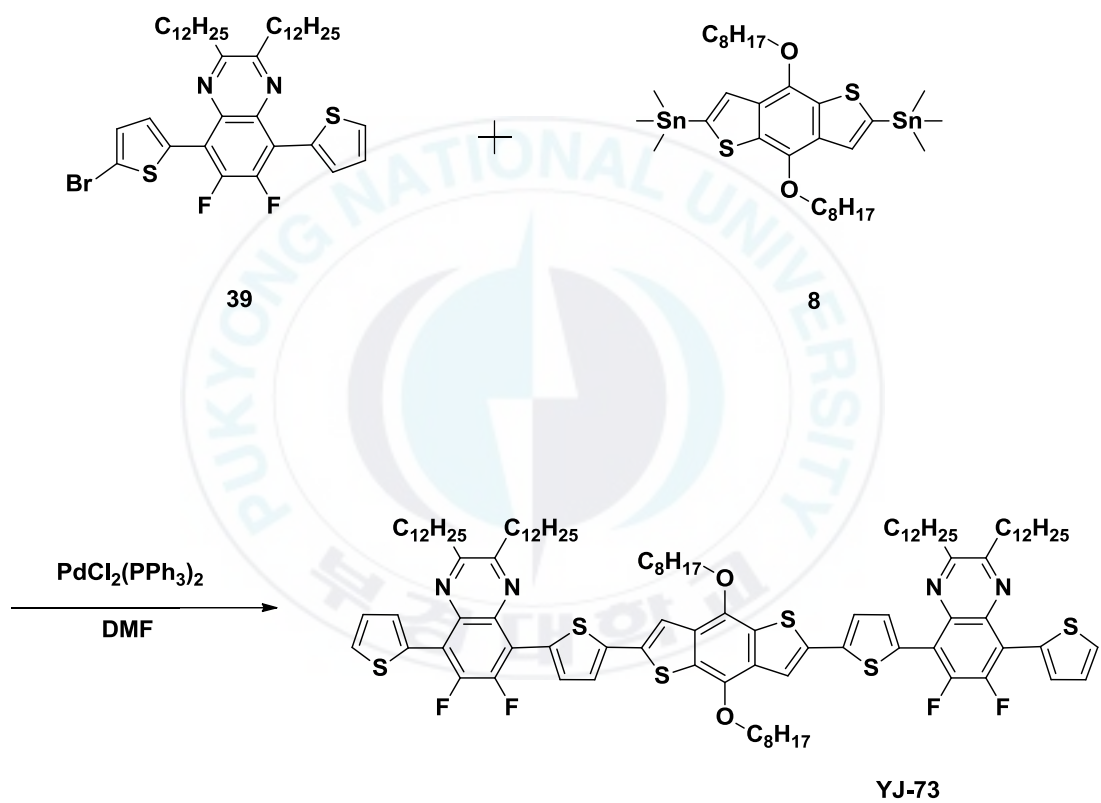
In a 100 mL dry flask, 5-(5-bromothiophen-2-yl)-2,3-dihexcyl-6,7-difluoro-8-(thiophen-2-yl)quinoxaline (**41**) (0.618 g, 1.07 mmol), (4,8-bis((2-ethylhexyl)oxy)benzo[1,2-*b*:4,5-*b'*])dithiophene-2,6-diyl)bis(trimethylstannane) (**6**) (0.346 g, 0.448 mmol) and bis(triphenylphosphine) palladium(II) dichloride (7.0 mg, 0.0107 mmol) were dissolved in *N,N*-dimethylformamide (10 mL) under argon atmosphere. And then, the mixture was stirred at 85~90 °C overnight. And then, the mixture was extracted with chloroform (CHCl<sub>3</sub>). The organic phase was washed with water and dried over anhydrous MgSO<sub>4</sub>. The solvent was removed by rotary evaporation and the residue was purified by silica column with petroleum hexane/CH<sub>2</sub>Cl<sub>2</sub> (6:1) to give a red solid of **YJ-72** (0.38 g, 58.90%).



**Scheme 19.** Synthetic route of EH-BDT(DTDFDHexQx)<sub>2</sub> (YJ-72).

**II-4-11. Synthesis of 8,8'-(5,5'-(4,8-bis(octyloxy)benzo[1,2-*b*:4,5-*b*']dithiophene-2,6-diyl)bis(thiophene-5,2-diyl))bis(2,3-didodecyl-6,7-difluoro-5-(thiophen-2-yl)quinoxaline (YJ-73)**

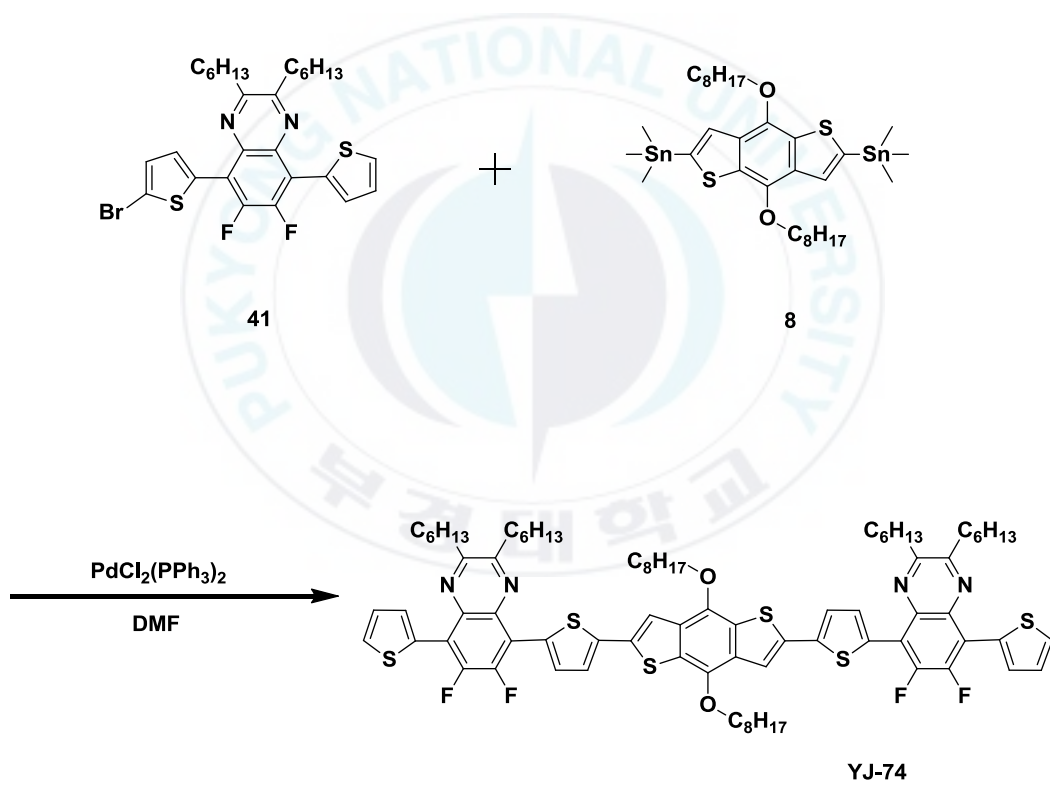
In a 100 mL dry flask, 5-(5-bromothiophen-2-yl)-2,3-didodecyl-6,7-difluoro-8-(thiophen-2-yl)quinoxaline (**39**) (0.67 g, 0.89 mmol), (4,8-bis(octyloxy)benzo[1,2-*b*:4,5-*b*']dithiophene-2,6-diyl)bis(trimethylstannane) (**8**) (0.3 g, 0.38 mmol) and bis(triphenylphosphine) palladium(II) dichloride (6.2 mg, 0.0089 mmol) were dissolved in *N,N*-dimethylformamide (10 mL) under argon atmosphere. And then, the mixture was stirred at 85~90 °C overnight. And then, the mixture was extracted with chloroform (CHCl<sub>3</sub>). The organic phase was washed with water and dried over anhydrous MgSO<sub>4</sub>. The solvent was removed by rotary evaporation and the residue was purified by silica column with petroleum hexane/CH<sub>2</sub>Cl<sub>2</sub> (6:1) to give a red solid of **YJ-73** (0.391 g, 57.91%).



**Scheme 20.** Synthetic route of Oct-BDT(DTDFDDoQx)<sub>2</sub> (**YJ-73**).

**II-4-12. Synthesis of 8,8'-(5,5'-(4,8-bis(octyloxy)benzo[1,2-*b*:4,5-*b'*])dithiophene-2,6-diyl)bis(thiophene-5,2-diyl))bis(2,3-dihexyl-6,7-difluoro-5-(thiophen-2-yl)quinoxaline (YJ-74)**

In a 100 mL dry flask, 5-(5-bromothiophen-2-yl)-2,3-dihexyl-6,7-difluoro-8-(thiophen-2-yl)quinoxaline (**41**) (0.618 g, 1.07 mmol), (4,8-bis(octyloxy)benzo[1,2-*b*:4,5-*b'*])dithiophene-2,6-diyl)bis(trimethylstannane) (**8**) (0.346 g, 0.448 mmol) and bis(triphenylphosphine) palladium(II) dichloride (7.0 mg, 0.0107 mmol) were dissolved in *N,N*-dimethylformamide (10 mL) under argon atmosphere. And then, the mixture was stirred at 85~90 °C overnight. And then, the mixture was extracted with chloroform (CHCl<sub>3</sub>). The organic phase was washed with water and dried over anhydrous MgSO<sub>4</sub>. The solvent was removed by rotary evaporation and the residue was purified by silica column with petroleum hexane/CH<sub>2</sub>Cl<sub>2</sub> (6:1) to give a red solid of **YJ-74** (0.421 g, 52.89%).



**Scheme 20.** Synthetic route of Oct-BDT(DTDFDHexQx)<sub>2</sub> (**YJ-74**).

## Chapter III. Results and Discussion

### III-1. Polymerization Results

The similar solubility was shown among two polymers. YJ-61 and YJ-62 can be dissolved partially in chloroform, toluene, but perfectly be dissolved in chlorobenzene and 1,2-dichlorobenzene (o-DCB) at elevated temperature. The weight-average molecular weight ( $M_w$ ), number- average molecular weight ( $M_n$ ), and polydispersity (PDI) were estimated by gel permeation chromatography (GPC) at room temperature with chloroform as an eluent (Table III-1). Since two polymers had poor solubility in chloroform at room temperature, it could not be accurately analyzed.

**Table III-1.** Polymerization Results.

Polymers	$M_n^a$	$M_w^a$	PDI <sup>a</sup>
YJ-61	6872	9150	1.33
YJ-62	1194	2544	2.13

<sup>a</sup>Number-average molecular weight ( $M_n$ ), weight-average molecular weight ( $M_w$ ) and polydispersity of the polymers were determined by gel permeation chromatography (GPC) in chloroform using polystyrene standards.

### III-2. Thermal Stability of Polymers and Small Molecules

Thermal stability is essential for material for photovoltaic devices because it is exposed with sun light. Over the 300 °C of 5% weight loss temperature ( $T_d$ ), these materials have a stability against exposure of sun light. Thermal properties of two polymers (YJ-61, YJ-62) and small molecules (YJ-63 ~ YJ-74) were measured by TGA methods (Figures III-1, Table III-2). All materials showed over 318 °C of  $T_d$  value. Therefore, all materials had good thermal stability.

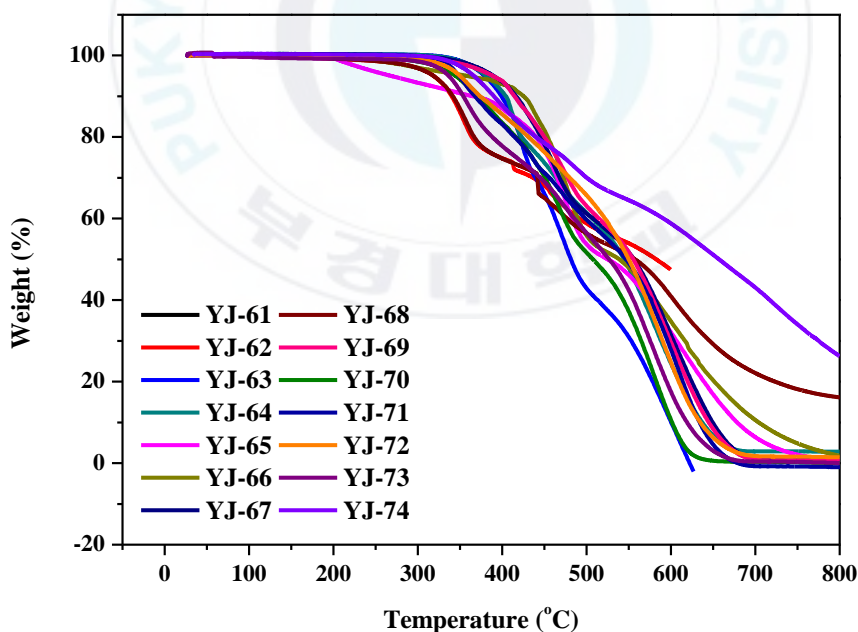


**Figure III-1.** Thermo gravimetric analysis of materials.

**Table III-2.**Decomposition Temperatures of Materials.

Materials	YJ - 61	YJ - 62	YJ - 63	YJ - 64	YJ - 65
$T_d$ (°C)	320	318	379	381	350
Materials	YJ - 66	YJ - 67	YJ - 68	YJ - 69	YJ - 70
$T_d$ (°C)	358	389	318	388	344
Materials	YJ - 71	YJ - 72	YJ - 73	YJ - 74	
$T_d$ (°C)	349	350	336	366	

Onset decomposition temperatures ( $T_d$ ) (5% weight loss) measured by TGA under Air

### III-3. Optical Properties of Polymers and Small Molecules

#### III-3-1. Optical Properties of Polymers

Absorption spectra of two polymers in chloroform solution and in solid film were shown in Figure III-2 and Figure III-3, respectively. The absorption spectra in solution had maximum peaks at 800 and 718 nm and in solid film had maximum peaks at 800 and 655 nm in YJ-61, YJ-62, respectively. As shown these results, YJ-62 containing more thiophene unit in polymer backbone was blue-shifted. It was accordance with the result of A-A type polymer solar cell that our lab made before. The optical bandgap ( $E_g^{opt}$ ) inferred from the onset

(867~829 nm) of the polymer absorption edges in the films is 1.47~1.54 eV. It is well known for the small bandgap of a polymer in field of BHJ solar cells.

**Table III-3.** Optical Properties of Polymers.

polymer	Abs.			$E_g^{opt}$ (eV)
	solution <sup>a</sup>	film		
	$\lambda_{max}$ (nm)	$\lambda_{max}$ (nm)	$\lambda_{edge}$ (nm)	
YJ - 61	800	800	867	1.47
YJ - 62	718	655	829	1.54

<sup>a</sup> In CF solution.

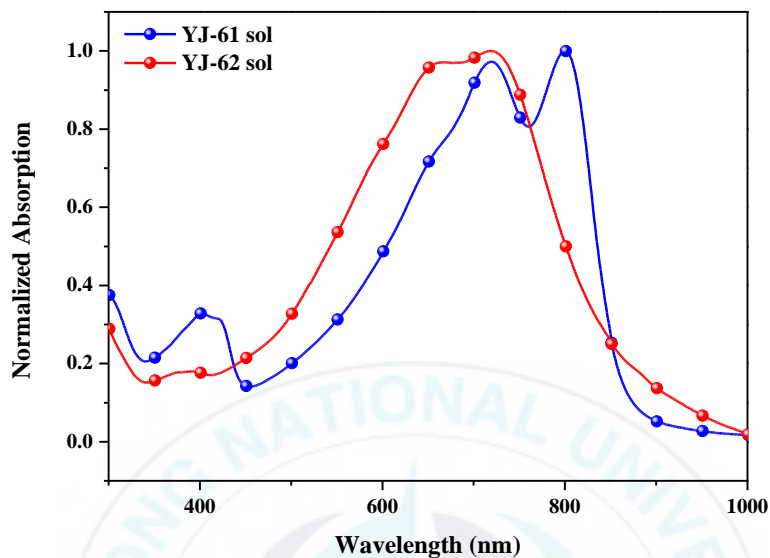


**Figure III-2.** UV-visible absorption spectra of polymers in chloroform.

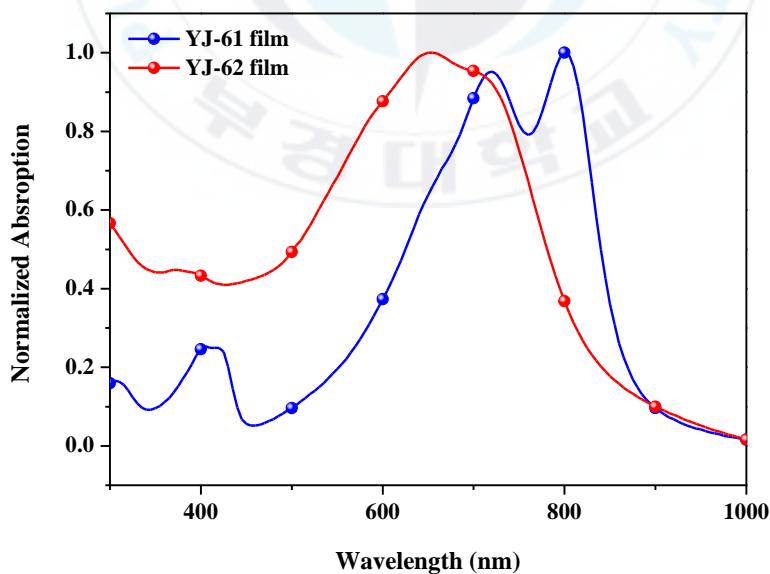


**Figure III-3.** UV-visible absorption spectra of polymers in a thin film formed via spin-cast from a solution in chloroform (1wt%).

### III-3-2. Optical Properties of Small Molecule

Three series of small molecules (YJ-63 ~ YJ-68, YJ-69 ~ YJ-70, YJ-71 ~ YJ-74) was synthesized and optical properties was measured by UV-visible. As shown in Table III-4, Figure III-4 ~9, absorption spectra of YJ-63 ~ YJ 68 in film state show the bathochromic shift (about 28 nm ~ 72 nm at maximum peak) compared to in solution. These results showed that six small molecules all have intermolecular interaction and enhanced  $\pi$ - $\pi$  stacking in solid state. And there are two special point of this series. First of all, As shown in Table III-4, Figure III-6 ~9, thienothiophene (TT) substituted YJ-67 and YJ-68 showed more red-shifted  $\lambda_{\max}$  (475, 495 nm in solution, 516, 538 nm in film state) than bi-thiophene (bi-T) containing YJ-65 and YJ-66 (469, 479 nm in solution, 505,518 nm in film state). It was caused by more planar and rigid thieno-thiophene (TT) unit rather than bi-thiophene (bi-T). Therefore, materials based on TT have more fine intermolecular interaction and  $\pi$ - $\pi$  stacking than based on bi-T, which will be result in more bathochromic shift.<sup>40</sup> Secondly, in YJ-66 ~ 68, in case that alkyl group is oriented outward, It was more red-shifted than oriented inward. It may because of torsional energy. When orientation of alkyl group is outward, torsional energy decreased. Therefore, YJ-66, YJ-68 was more red shift than YJ-65, YJ-67.

Figure III-10 and Figure III-11 showed absorption spectra of YJ-69 and YJ-70.

In solution state,  $\lambda_{\max}$  of YJ-69 and YJ-70 spectra were located in 481, 465 nm

and bathochromic shift were taken in each film states about 11, 28 nm respectively.

The absorption spectra of YJ-71 ~ YJ-74 were exhibited in Figure III-12, Figure III-13. Since these series have similar backbone excluding alkyl chain, they showed similar  $\lambda_{\max}$  in solution (475, 471, 475 and 468 nm) and in film (538, 536, 538 and 540) state. And similarly other series, bathochromic shift was taken in film state (about 65 nm ~70 nm).

**Table III-4.** Optical Properties of Small Molecules.

polymer	Abs.			$E_g^{\text{opt}}$ (eV)
	solution <sup>a</sup>		film	
	$\lambda_{\max}$ (nm)	$\lambda_{\max}$ (nm)	$\lambda_{\text{edge}}$ (nm)	
YJ – 63	453	482	561	2.24
YJ – 64	426	454	525	2.40
YJ – 65	469	505	596	2.11
YJ – 66	479	518	605	2.08
YJ – 67	475	516	625	1.99
YJ - 68	495	538	643	1.93
YJ – 69	481	492	620	1.99
YJ – 70	465	493	574	2.19
YJ – 71	475	538	579	2.15
YJ – 72	471	536	582	2.13
YJ – 73	475	538	591	2.10
YJ - 74	468	540	592	2.10

<sup>a</sup> In CF solution.

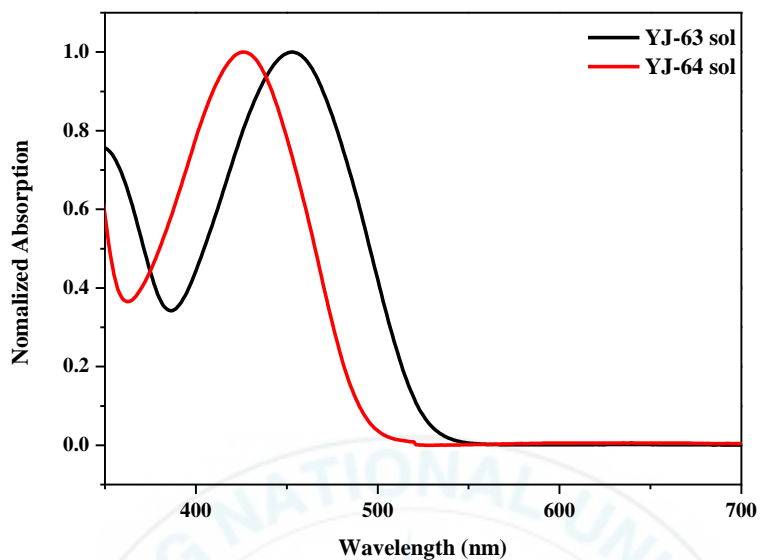


**Figure III-4.** UV-visible absorption spectra of YJ-63, YJ-64 in chloroform.

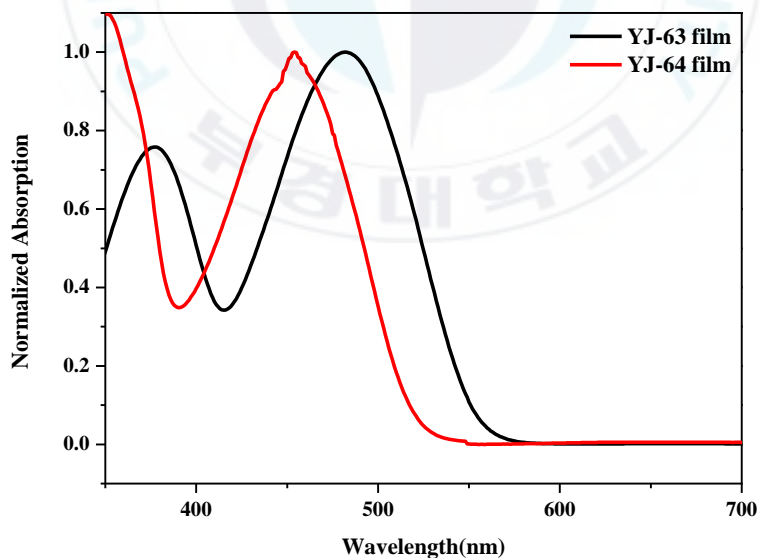


**Figure III-5.** UV-visible absorption spectra of YJ-63, YJ-64 in a thin film formed via spin-cast from a solution in chloroform (1 wt%).

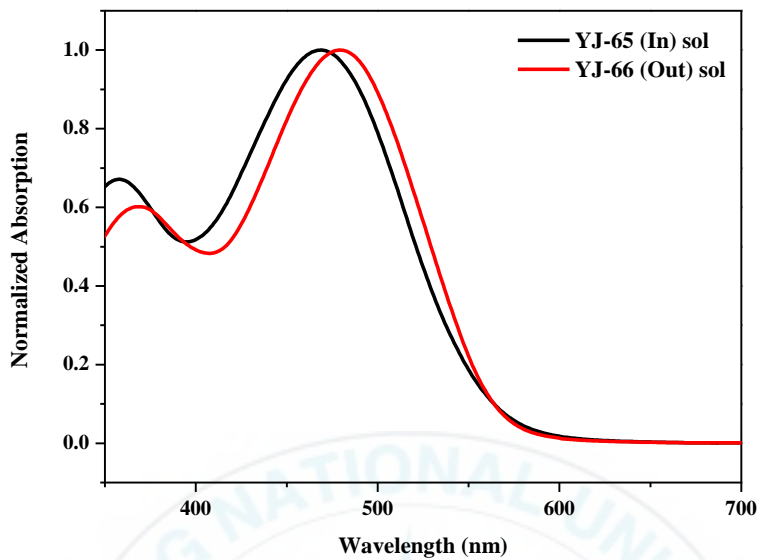


**Figure III-6.** UV-visible absorption spectra of YJ-65, YJ-66 in chloroform.

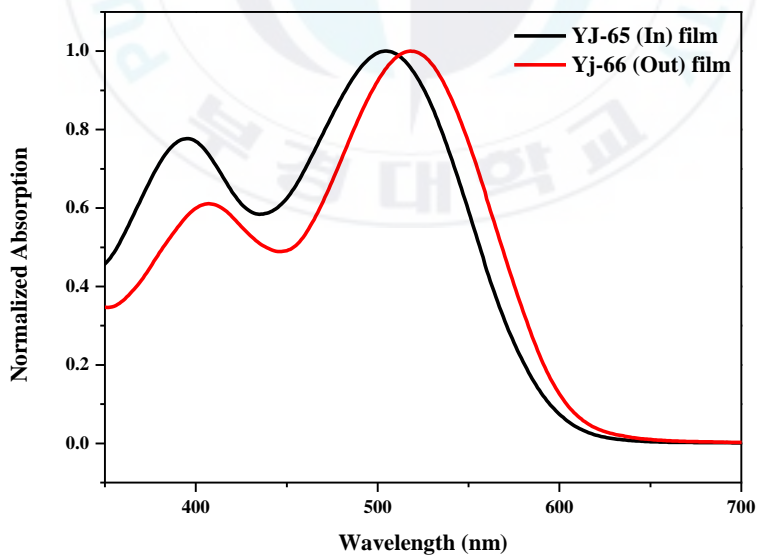


**Figure III-7.** UV-visible absorption spectra of YJ-65, YJ-66 in a thin film formed via spin-cast from a solution in chloroform (1wt%).

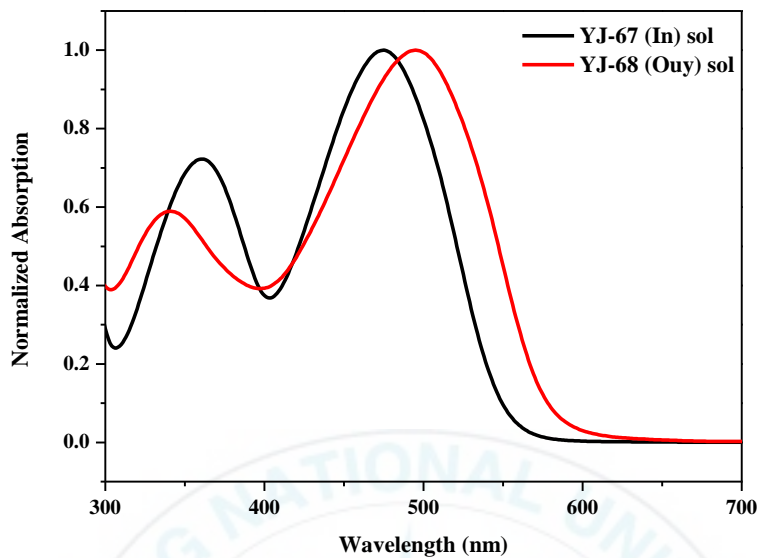


**Figure III-8.** UV-visible absorption spectra of YJ-67, YJ-68 in chloroform.

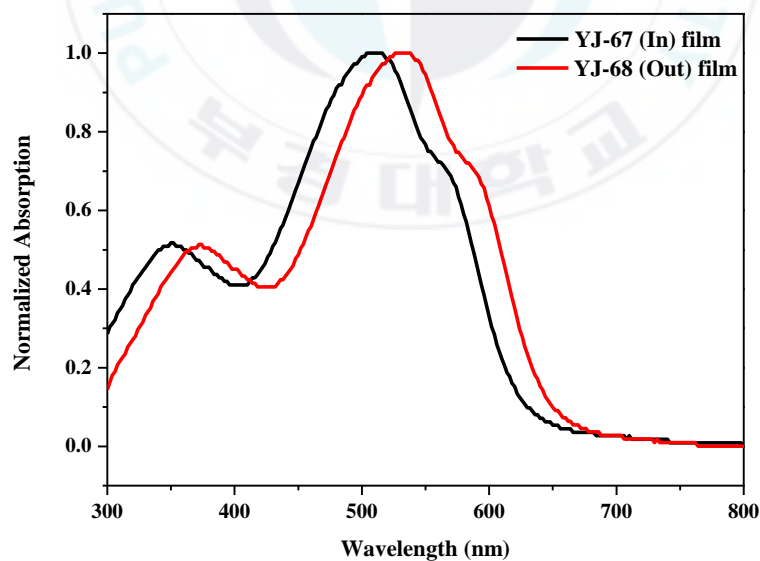


**Figure III-9.** UV-visible absorption spectra of YJ-67, YJ-68 in a thin film formed via spin-cast from a solution in chloroform (1 wt%).

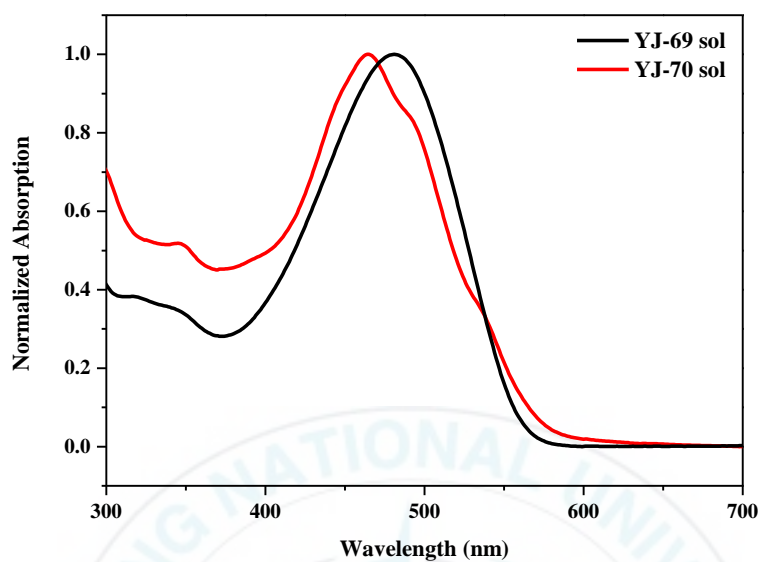


**Figure III-10.** UV-visible absorption spectra of YJ-69, YJ-70 in chloroform.

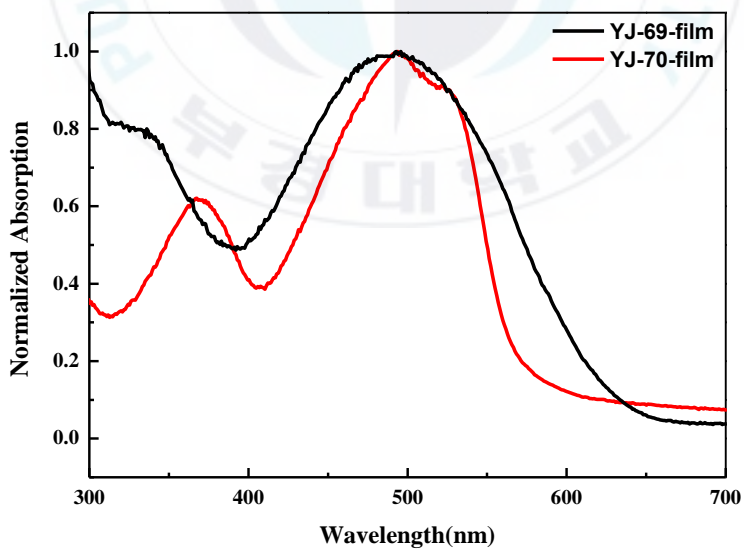


**Figure III-11.** UV-visible absorption spectra of YJ-69, YJ-70 in a thin film formed via spin-cast from a solution in chloroform (1wt%).

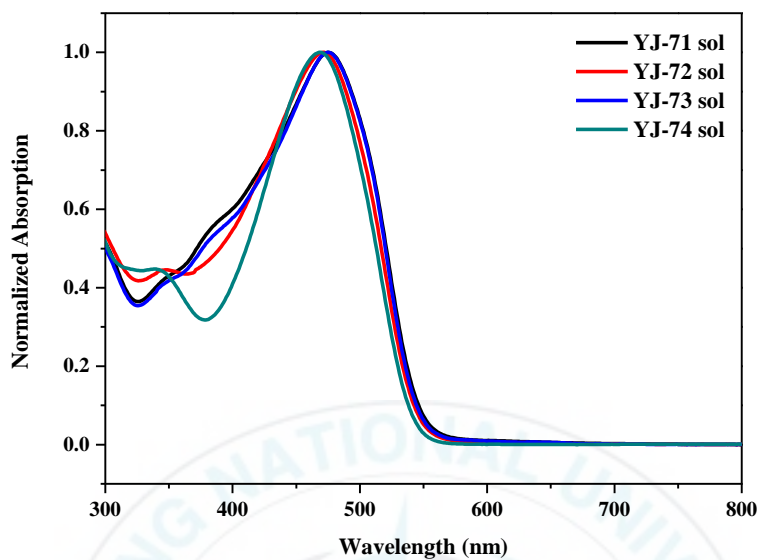


**Figure III-12.** UV-visible absorption spectra of YJ-71 ~ YJ-74 in chloroform.

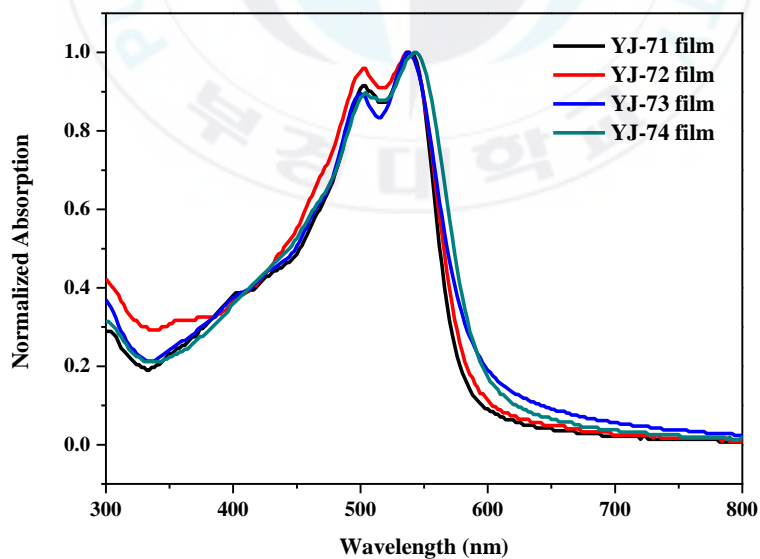


**Figure III-13.** UV-visible absorption spectra of YJ-71 ~ YJ-74 in a thin film formed via spin-cast from a solution in chloroform (1wt%).

### III-4. Electrochemical Properties of Materials.

Electrochemical properties such as the HOMO and LUMO energy levels of resulting materials were measured by cyclic voltammetry. The HOMO energy level was deduced from  $E_{\text{ox}}^{\text{onset}}$  and the LUMO energy level was from some equation using  $E_{\text{re}}^{\text{onset}}$  and  $E_{\text{ox}}(\text{ferrocene})$ . This equation is followed below.

$$\text{HOMO} = -(E_{\text{ox}}^{\text{onset}} - E_{\text{ox}}(\text{ferrocene})) - 4.8 \text{ (eV)}$$

$$\text{LUMO} = -(E_{\text{re}}^{\text{onset}} - E_{\text{ox}}(\text{ferrocene})) - 4.8 \text{ (eV)}$$

Two polymers (YJ-61 and YJ-62) showed narrow optical bandgap (1.47, 1.54 eV), but HOMO energy level somewhat high (-5.00, -5.08). Since  $V_{\text{oc}}$  value is related to difference in HOMO energy level of donor unit and LUMO energy level of acceptor unit, it would result in bad  $V_{\text{oc}}$  and bad performance. And YJ-66 and YJ-68 had deeper HOMO energy level (-5.31, -5.32) and LUMO energy level (-2.92, -3.06) rather than YJ-65 and YJ-67. (HOMO; -5.25, -5.20, LUMO; -2.89, -2.87). The orientation of alkyl group and hindrance would be attributed to intermolecular packing and altered energy levels. And YJ-69 displayed more deep HOMO, LUMO energy level (-5.33, -2.86) than YJ-70 (-5.20, -2.70).

And since, YJ-71, YJ-72, YJ-73 and YJ-74 had same backbone except for alkyl chain, so this series showed similar electrochemical properties, but they showed

some difference in HOMO energy level. In case that ethyl-hexyl group was substituted on BDT backbone (YJ-71, YJ-72), It had more deep HOMO energy level (-5.38, -5.35) than octyl chain substituted on BDT backbone (YJ- 73, YJ-74; -5.27, -5.29)



**Table III-5.** Electrochemical properties of the materials.

Materials	CV		
	HOMO (eV)	LUMO (eV)	$E_g^{ec}$ (eV)
YJ-61	-5.00	-3.18	1.82
YJ-62	-5.08	-2.97	2.11
YJ-63	-5.25	-2.82	2.43
YJ-64	-5.32	-2.83	2.49
YJ-65	-5.25	-2.89	2.36
YJ-66	-5.31	-2.92	2.39
YJ-67	-5.20	-2.87	2.34
YJ-68	-5.32	-3.06	2.26
YJ-69	-5.33	-2.86	2.47
YJ-70	-5.20	-2.70	2.55
YJ-71	-5.38	-2.91	2.47
YJ-72	-5.35	-2.93	2.42
YJ-73	-5.27	-2.93	2.34
YJ-74	-5.29	-2.92	2.37

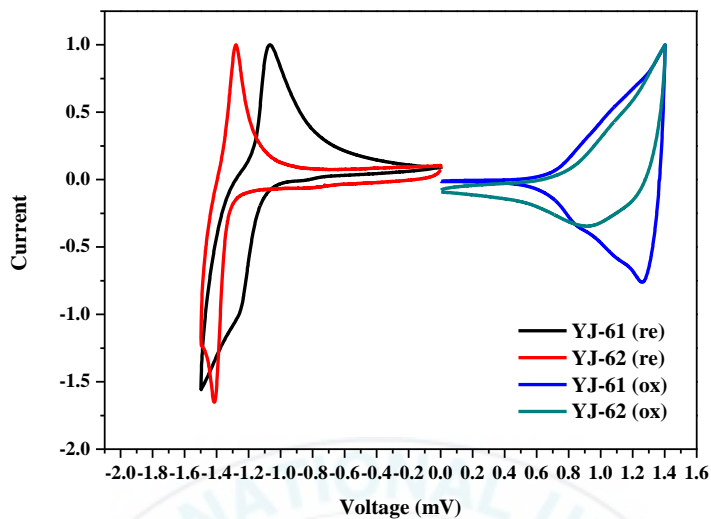


**Figure III-14.** Cyclic voltammetry curves of YJ-61, YJ-62 in 0.1 M  $\text{Bu}_4\text{NPF}_6$  acetonitrile solution at a scan rate of 100 mV/s at room temperature (vs an Ag quasi-reference electrode).

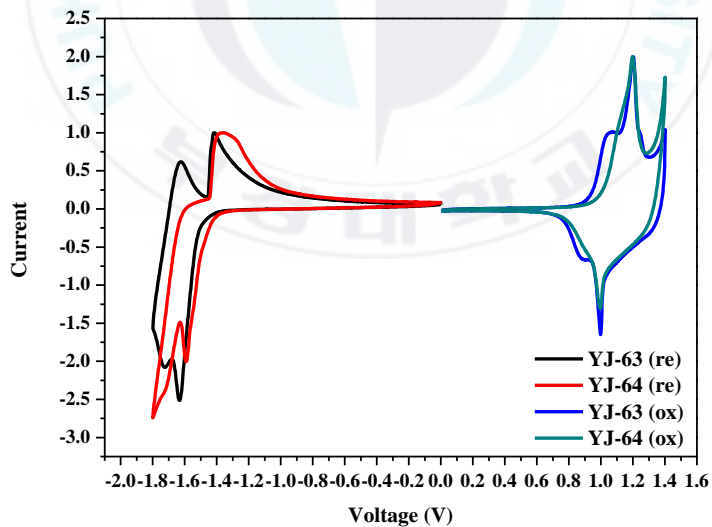


**Figure III-15.** Cyclic voltammetry curves of YJ-63, YJ-64 in 0.1 M  $\text{Bu}_4\text{NPF}_6$  acetonitrile solution at a scan rate of 100 mV/s at room temperature (vs an Ag quasi-reference electrode).

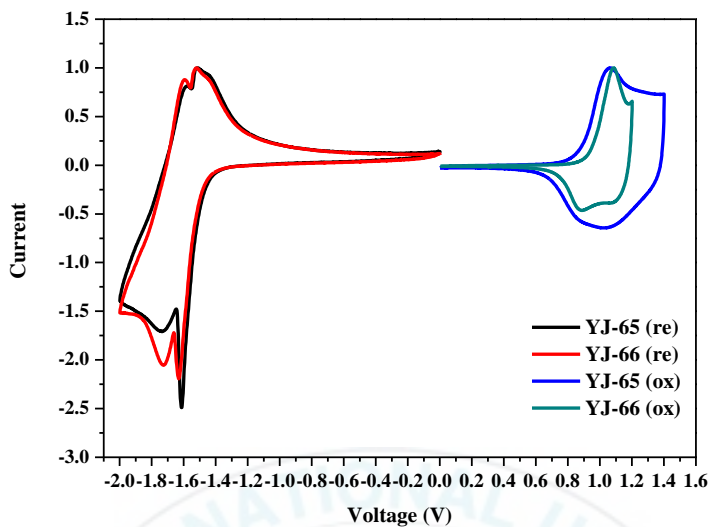


**Figure III-16.** Cyclic voltammetry curves of YJ-65, YJ-66 in 0.1 M  $\text{Bu}_4\text{NPF}_6$  acetonitrile solution at a scan rate of 100 mV/s at room temperature (vs an Ag quasi-reference electrode).

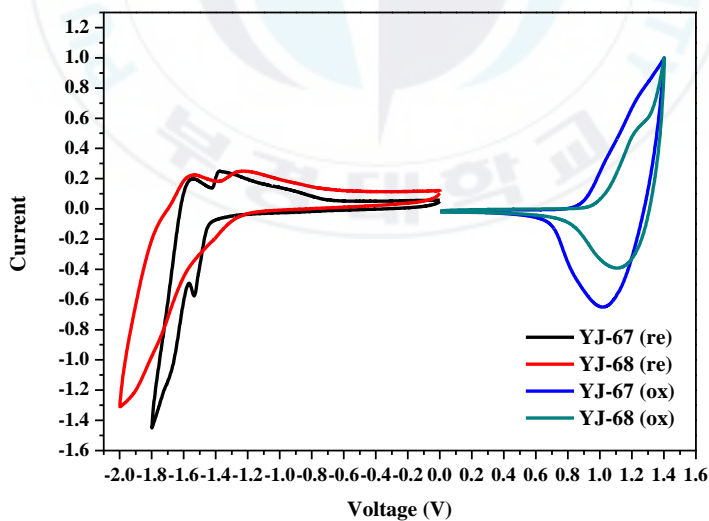


**Figure III-17.** Cyclic voltammetry curves of YJ-67, YJ-68 in 0.1 M  $\text{Bu}_4\text{NPF}_6$  acetonitrile solution at a scan rate of 100 mV/s at room temperature (vs an Ag quasi-reference electrode).

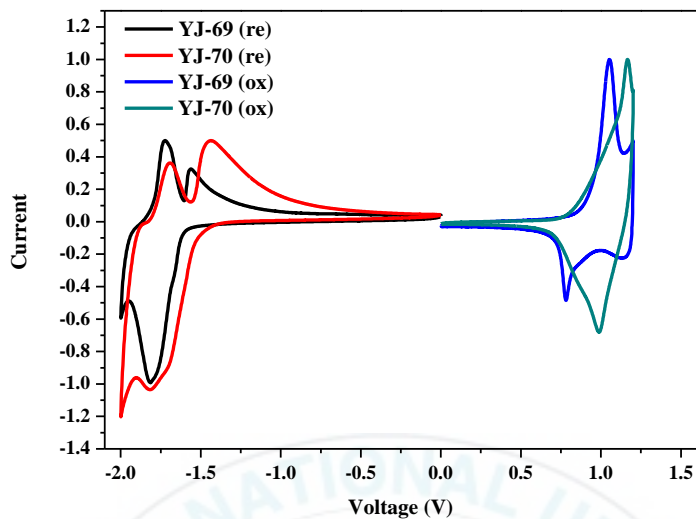


**Figure III-18.** Cyclic voltammetry curves of YJ-69, YJ- 70 in 0.1 M  $\text{Bu}_4\text{NPF}_6$  acetonitrile solution at a scan rate of 100 mV/s at room temperature (vs an Ag quasi-reference electrode).

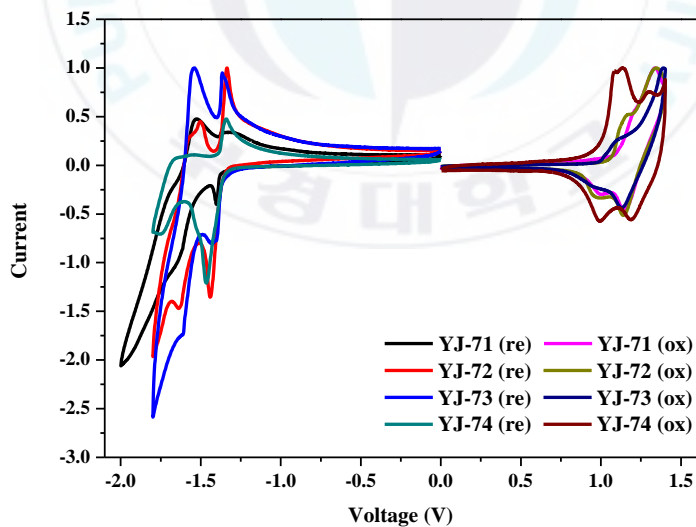


**Figure III-19.** Cyclic voltammetry curves of YJ-71, YJ-72, YJ-73 and YJ-74 in 0.1 M  $\text{Bu}_4\text{NPF}_6$  acetonitrile solution at a scan rate of 100 mV/s at room temperature (vs an Ag quasi-reference electrode).

### III-4. Photovoltaic Properties of Materials

The PCE of 0.01 ~ 0.87% was achieved in the solar cell devices of fourteen materials (two polymers and twelve small molecules) mixed with PC<sub>70</sub>BM in 1:1.5 or 1:1 ratio and 3% of DIO additive as displayed in Table III-6. In two polymers, YJ-61 showed somewhat high value of  $J_{sc}$  7.40 mA/cm<sup>2</sup>. It was caused by broad UV-vis absorption region, which effect the light absorption. On the other hand, YJ-62 had a poor solubility in common solvent like chloroform, toluene and chlorobenzene. Therefore, device based on YJ-62 could not make to measure photovoltaic properties. Since the HOMO level of donor material is related with  $V_{oc}$ , YJ-61 had somewhat low  $V_{oc}$  value 0.50 V. In small molecules, especially YJ-63 ~ YJ-68, the PCE was achieved 0 ~ 0.13%. Among them, YJ-66 and YJ-68 displayed somewhat high PCE 0.11 and 0.13, respectively. These results was in line with optical and electrochemical properties. YJ-69 and YJ-70 blended device could not be measured exactly due to the poor solubility in common solvents. In YJ-71 ~ YJ-74 series, the PCE was measured 0.23 ~ 0.62%. Among them, YJ-71 having more long alkyl chain in Qx unit and bulky side chain in BDT unit showed highest PCE 0.62%. This results caused by solubility of more long side chain and docking effect with PCBM of bulky side chain.

**Table III-6.** Photovoltaic Performance of Solar Cells Based on YJ-61 ~ YJ-74.

Materials	$J_{sc}$ (mA/cm <sup>2</sup> )	$V_{oc}$ (V)	FF	PCE (%)
YJ-61	7.40	0.50	0.22	0.87
YJ-62	0	0	0	0
YJ-63	0.73	0.55	0.29	0.11
YJ-64	0.00	0.05	0.00	0
YJ-65	0.48	0.54	0.32	0.07
YJ-66	0.47	0.75	0.27	0.11
YJ-67	0.11	0.44	0.23	0.01
YJ-68	0.70	0.62	0.31	0.13
YJ-69	0.88	0.08	0.24	0.02
YJ-70	0.21	0.42	0.30	0.03
YJ-71	2.30	0.83	0.32	0.62
YJ-72	3.07	0.55	0.32	0.36
YJ-73	1.08	0.66	0.32	0.23
YJ-74	2.10	0.61	0.32	0.41

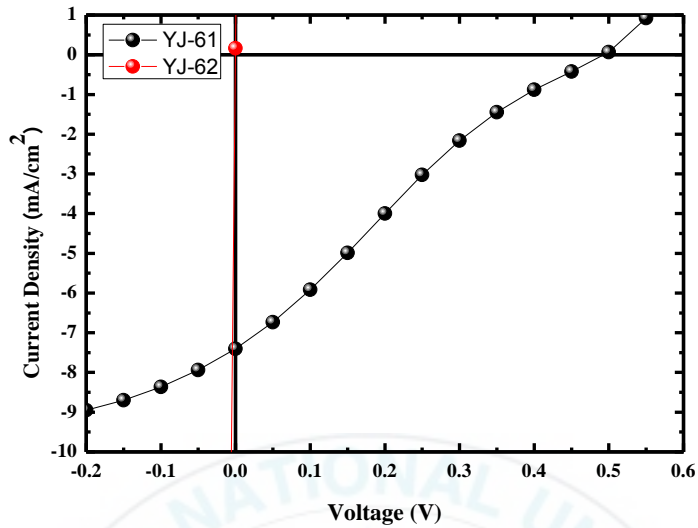


**Figure III-20.** J-V curves of the solar cell devices based on YJ-61, YJ-62 under  $100\text{mW} / \text{cm}^2$  AM 1.5G illumination.

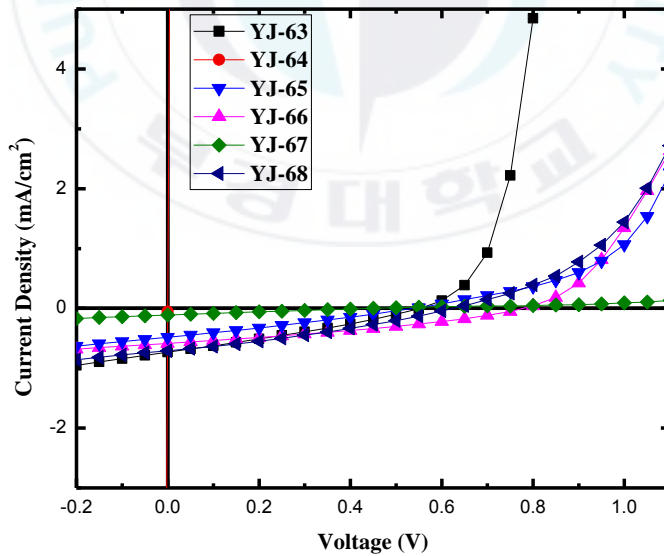


**Figure III-21.** J-V curves of the solar cell devices based on YJ-63 ~ YJ-68 under  $100\text{mW} / \text{cm}^2$  AM 1.5G illumination.

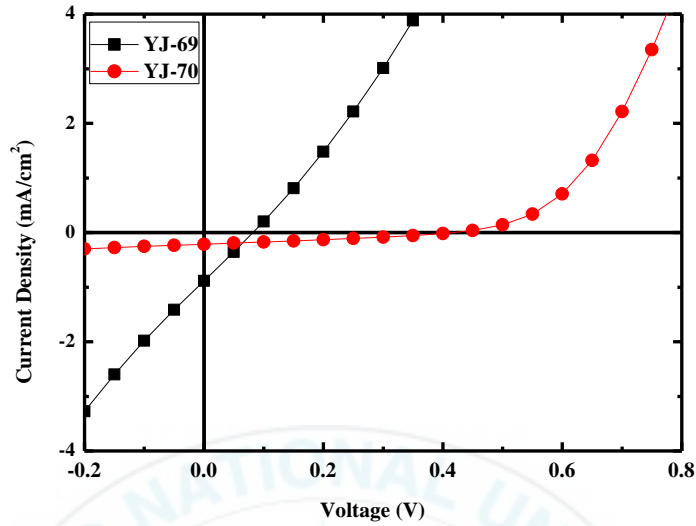


**Figure III-22.** J-V curves of the solar cell devices based on YJ-69, YJ-70 under  $100\text{mW} / \text{cm}^2$  AM 1.5G illumination.

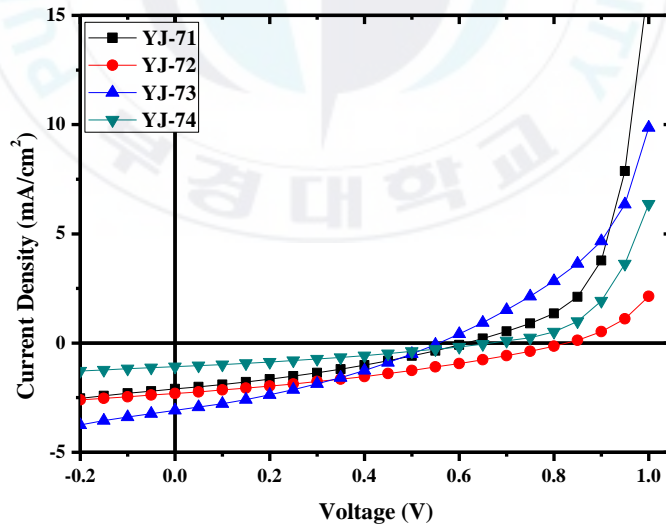


**Figure III-23.** J-V curves of the solar cell devices based on YJ-71 ~ YJ-74 under  $100\text{mW} / \text{cm}^2$  AM 1.5G illumination.

## Chapter IV. Conclusions

In summary, new A-A type two conjugated polymers based on bithiazole (bi-Tz) and di-fluorinated quinoxaline (DFQx) unit and twelve small molecules of three types including DFQx, benzodithiophene (BDT) and thiophene derivatives were synthesized via stille coupling. In the two polymers, YJ-61 and YJ-62, bi-Tz and DFQx unit was used as acceptor unit. These two polymers was synthesized to look into effect of polymers containing two acceptor unit. Resultingly, A-A type polymers showed broad absorption spectra, it leded to somewhat high  $J_{sc}$ . In YJ-63 ~ 68 series, especially YJ-65, 66 and YJ-67, YJ-68, orientation of side chain affected electrochemical, optical and finally photovoltaic properties. The material with side chain outward had more red shift absorption spectra and deeper HOMO level than those with inward. In conclusion, material with side chain outward had better  $J_{sc}$ ,  $V_{oc}$  and PCE. In YJ-71 ~ 74 series, YJ-71 : PC<sub>70</sub>BM blending device exhibited the best performance with a  $V_{oc}$  of 0.83 V,  $J_{sc}$  of 2.30 mA/cm<sup>2</sup>, FF of 0.32% and PCE of 0.62%. YJ-71 had longer alkyl side chain and bulky alkyl side chain. Long alkyl side chain would affect solubility and bulky alkyl side chain had good docking effect with acceptor materials rather than liner alkyl chain. It resulted in YJ-71 with best performance. Overall, this paper suggests that the orientation of alkyl side chain, suitable alkyl side chain, and what kind of thiophene derivatives can affect the performance of the PSCs.

## References

- [1] Liu, Y.; Zhao, J.; Li, Z.; Mu, C.; Ma, W.; Hu, H.; Jiang, K.; Lin, H.; Ade, H.; Yan, H. *Nat. Commun.* **2014**, DOI: 10.1038/ncomms6293.
- [2] Hou, J.; Chen, H.-Y.; Zhang, S.; Li, G.; Yang, Y. *J. Am. Chem. Soc.* **2008**, 130, 16144-16145.
- [3] Subbiah, J.; Purushothaman, B.; Chen, M.; Qin, T. S.; Gao, M.; Vak, D.; Watkins, S. E.; Wilson, G. J.; Holmes, A. B.; Wong, W. W. H.; Jones, D. J. *Adv. Mater.* **2015**, 27, 702-705.
- [4] Qun Wan, Xia Guo, Zaiyu Wang, Wanbin Li, Bing Guo, Wei Ma, MaoJie Jhang, Yongfang Li. *Adv. Funct. Mater.* **2016**, 26, 6634-6640.
- [5] Shaoqing Zhang, Long Ye, Jianhui Hou. *Adv. Energy Mater.* **2016**, 6, 1502529
- [6] Yaocheng Jin, Zhiming Chen, Sheng Dong, Nannan Zheng, Lei Ying, Xiao-Fang Jiang, Feng Liu, Fei Huang, Yong Cao. *Adv. Mater.* **2016**, 28, 9511-9818.
- [7] Jingbi You, Letian Dou, Takehito Kato, Kenichiro Ohya, Keith Emery, Chun-Chao Chen, Jing Gao, Gang Li, Yang, Y. *Nat. Commun.* **2013**, 4, 1446
- [8] Tang, Ailing; Zhan, Chuanlang; Yao, Jiannian. *Adv. Energy Mater.* **2015**, 5(13), n/a
- [9] Ailing Tang, Chuanlang Zhan, Jiannian Yao. *Adv. Energy Mater.* **2015**, 5,

1500059.

- [10] Qian Zhang, Bin Kan, Feng Liu, Xiaoqing Chen, Yi Zuo, Wang Ni, Miaomiao Li, Fei Huang, Yong Cao, Ziqi Liang, Thomas P. Russell, Yongsheng Chen. *Nat. Photonics*. **2014**, DOI:10.1038/NPHOTON.2014.269
- [11] Ke Gao, Lisheng Li, Tianqi Lai, Fei Huang, Junbiao Peng, Yong Cao, Thomas P. Russell, Rene A. J. Janssen, Xiaobin Peng. *J. Am. Chem. Soc.* **2015**, 137, 7282-7285.
- [12] C. Winder, N. S. Sariciftci, *J. Mater. Chem.* **2004**, 14, 1077.
- [13] Weickert, J., Dunbar, R. B., Hesse, H. C., Wiedemann, W. & Schmidt-Mende, L. Nanostructured organic and hybrid solar cells. *Adv. Mater.* **2011**, 23, 1810–1828.
- [14] Wudl, F. & Srdanov, G. *US patent*. **1993**, 5, 189, 136.
- [15] Brabec, C. J., Shaheen, S. E., Winder, C., Sariciftci, N. S. & Denk, P. *Appl. Phys. Lett.* **2002**, 80, 1288–1290.
- [16] Wienk, M. M. et al. *Angew. Chem. Int. Ed.* **2003**, 42, 3371–3375
- [17] Bao, Z., Dodabalapur, A. & Lovinger, A. J. *Appl. Phys. Lett.* **1996**, 69, 4108–4110
- [18] M. C. Scharber, D. Mühlbacher, M. Koppe, P. Denk, C. Waldauf, A. J. Heeger, C. Brabec, J. *Adv. Mater.* **2006**, 18 (6), 789-794.

- [19] M. D. Perez, C. Borek, S. R. Forrest, M. E. Thompson, *J. Am. Chem. Soc.* **2009**, 131 (26), 9281-9286.
- [20] K. Vandewal, K. Tvingstedt, A. Gadisa, O. Inganäs, J. V. Manca, *Nature Mater.* **2009**, 8 (11), 904-909.
- [21] Moliton, A.; Nunzi, J.-M.; *Polym. Int.* **2006**, 55 (6), 583-600
- [22] Shaoqing Zhang, Yunpeng Qin, Wenchao Zhao, Han Young Woo, Jianhui Hou. *Macromolecules.* **2016**, 49, 2993-3000.
- [23] Haijun Bin, Zhi-Guo Zhang, Lian Zhong, Changduk Yang, Yongfang Li. *J. Am. Chem. Soc.* **2016**, 138, 4657-4664.
- [24] Chen, D., Liu, F., Wang, C., Nakahara, A. & Russell, T. P., *Nano Lett.* **2011**, 11, 2071–2078
- [25] L. Dou , Y. Liu , Z. Hong , G. Li , Y. Yang , *Chem. Rev.* **2015** , 115 , 12633 ;
- [26] J. D. Zimmerman , V. V. Diev , K. Hanson , R. R. Lunt , E. K. Yu , M. E. Thompson , S. R. Forrest , *Adv. Mater.* **2010**, 22, 2780 ;
- [27] X. Zhao , Y. Wen , L. Ren , L. Ma , Y. Liu , X. Zhan , *J. Polym.Sci., Part A: Polym. Chem.* **2012**, 50 , 4266 ;
- [28] Xiaofen Wang, Lei lv, Cuozen Shen, Zhou Yang, *Adv. Func. Mater.* **2016**, 26, 6306-6015;
- [29] Ke Gao, Lisheng Li, Tianqi Lai, Xiaobin Peng, *J. Am. Chem. Soc.* **2015**, 137, 7282-7285 ;
- [30] Zhou, H.; Yang, L.; Price, S. C.; Knight, K. J.; You, W. *Angew. Chem., Int.*

- Ed.* **2010**, 49, 7992.
- [31] Zhou, H.; Yang, L.; Stoneking, S.; You, W. *ACS Appl. Mater. Interfaces*, **2010**, 2, 1377.
- [32] He, Z.; Zhong, C.; Su, S.; Xu, M.; Wu, H.; Cao, Y. *Nat. Photonics*, **2012**, 6, 591.
- [33] Liao, S.-H.; Jhuo, H.-J.; Cheng, Y.-S.; Chen, S.-A. *Adv. Mater.* **2013**, 25, 4766.
- [34] S. C. Price, A. C. Stuart, L. Q. Yang, H. X. Zhou and W. You, *J. Am. Chem. Soc.* **2011**, 133, 4625-4631;
- [35] L. Huo, J. Hou, S. Zhang, H.-Y. Chen, Y. Yang, *Angew. Chem., Int. Ed.* **2010**, 49 (8), 1500-1503;
- [36] H. Zhou, L. Yang, A. C. Stuart, S. C. Price, S. Liu, W. You, *Angew. Chem., Int. Ed.* **2011**, 50 (13), 2995-2998;
- [37] H. Zhou, L. Yang, S. C. Price, K. J. Knight, W. You, *Angew. Chem., Int. Ed.* **2010**, 49 (43), 7992-7995;
- [38] X. Wang, E. Perzon, W. Mammo, F. Oswald, S. Admassie, N.-K. Persson, F. Langa, M. R. Andersson, O. Inganaes, *Thin Solid Films*, **2006**, 511-512 (1), 576-580;
- [39] J.-H. Tsai, C.-C. Chueh, M.-H. Lai, C.-F. Wang, W.-C. Chen, B.-T. Ko, C. Ting, *Macromolecules*, **2009**, 42 (6), 1897-1905;
- [40] Shaoqing Zhang, Bei Yang, Delong Liu, Qi wang, Chang He, Jianhui Hou.



## 감사의글

되 깊어본다면, 실험실 생활을 시작 한 게 엇그제 같은데 벌써 졸업을 앞두고 있다는 생각에 후련하다는 생각도 들지만, 씩씩하면서도 아쉬움도 많이 남습니다. 우선 2년 동안 저의 실험, 연구 그리고 그 뿐만 아니라 저를 한 명의 사회인으로서 인격체를 형성하는데 많은 도움을 주시고 잘 이끌어 주신 지도교수님 진영읍 교수님 정말 감사합니다. 그리고 저의 4년간의 학부생 시절, 그리고 2년간의 석사 생활 동안, 많은 도움과 조언을 아끼지 않으셨던 이근대 교수님, 문명준 교수님, 박성수 교수님, 손민영 교수님, 장동욱 교수님, 곽삼탁 교수님, 박진환 교수님 정말 감사의 인사 말씀을 드립니다. 그리고 같이 co work 하면서 측정을 도와주신 물리과 박성흠 교수님, 그리고 지훈이 형, 승민이 형 외 물리과 분들 감사합니다. 어려운 집안 형편에도 석사 진학을 허락하신 아버지, 어머니. 그리고 힘들 때 마다 나의 버팀목이 되어주었던 나의 여자친구 영숙이. 정말 정말 감사합니다. 그리고 학부생때부터 실험실 생활하면서 저에게 많은 도움을 주었던 동호 선배, 원준 선배, 영권이, 지현이, 상하 그리고 가람이... 항상 감사하게 생각하고 있습니다. 그리고 지금 YJ-lab 식구, 방장 하고 있는 원문이, 그리고 동환이 선배로써 많은 가르침을 주고, 항상 바른 모습만 보여주었어야 하는데 그러지 못해 많이 아쉽고 미안한 마음이 가득하네. 앞으로 남은 1년 좋은 성과 내길 바랄게. 그리고 이제 석사생활 시작하는 지현이 두 형님들 잘 보필하고 힘들겠지만 열심히 하고 그리고 얼마 보지 못한 우리 막둥이들 해송이랑 완수 실험실 생활하면서 많은 것 얻어가길 바랄게. 끝으로 다시 한번 모든 분들께 감사의 인사 말씀 드립니다.